XAFS facility at Indus-2 and results

S N Jha
Atomic & Molecular Physics Division, BARC
snjha@rrcat.gov.in

Schematic view of Indus complex

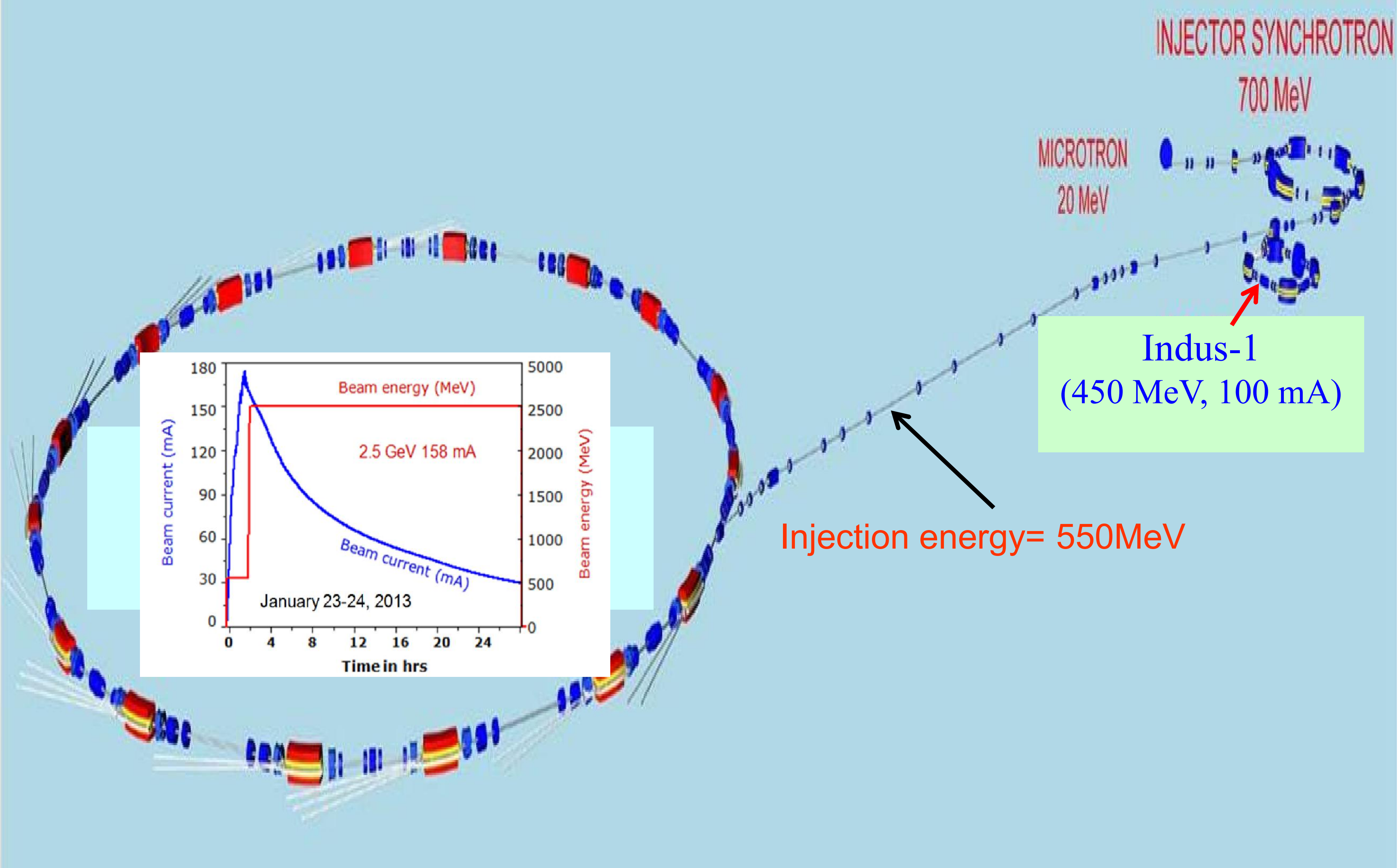

Layout of Indus-2 Beamlines

Total no. of beamline ports = 27

Ports for bending magnet beamlines = 22

12 Beamlines operational

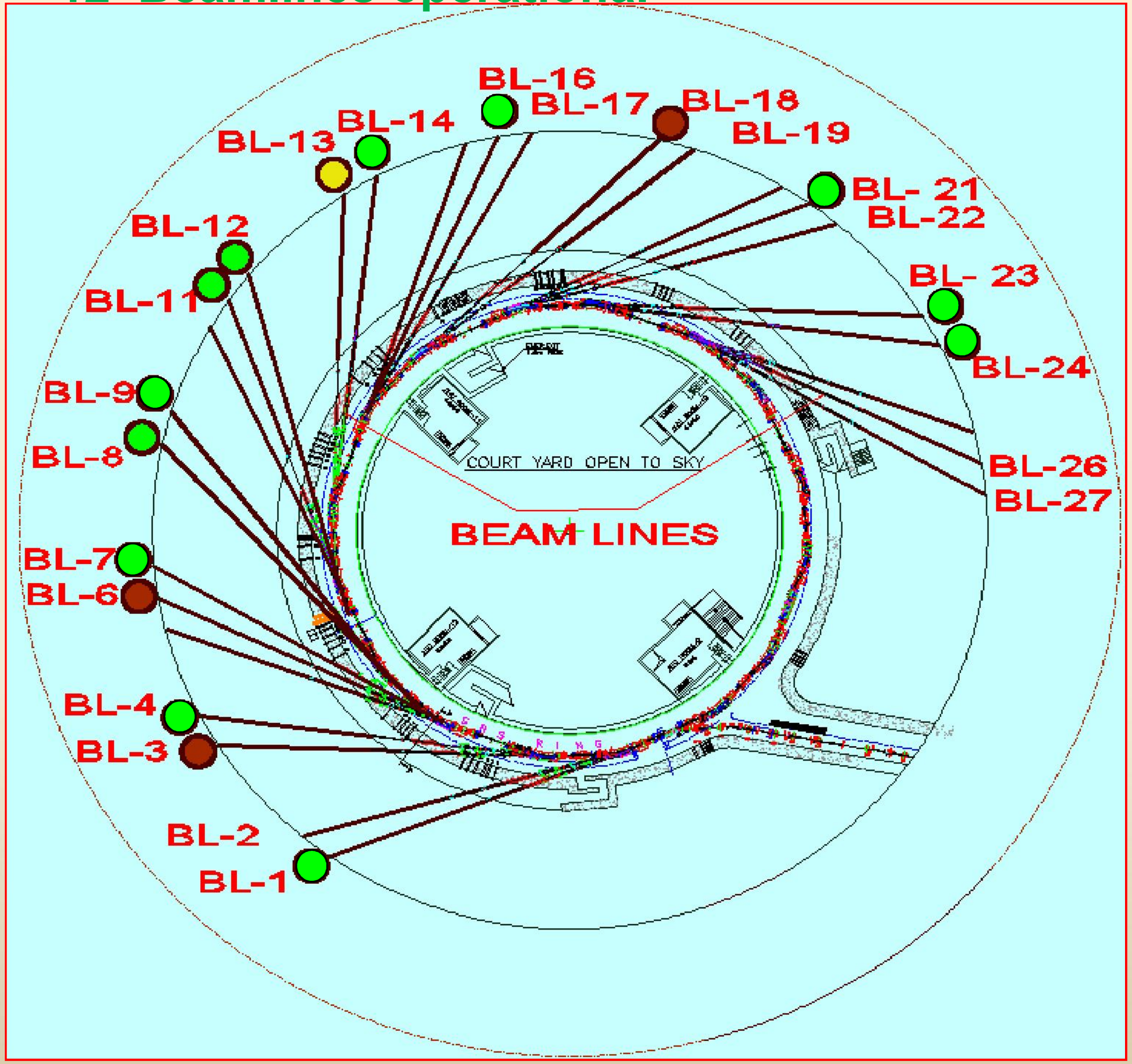

Operational	MCD/PES (BL-1)
Under development	Soft X-ray (BL-3)
Operational	Imaging (BL-4)
Under development	ARPES/PEEM (BL-6)
Operational	X-ray Lithography (BL-7)
Operational	Dispersive EXAFS (BL-8)
Operational	Scanning EXAFS (BL-9)
Operational	EDXRD (BL-11)
Operational	ADXRD(BL-12)
Under commissioning	GIXS(BL-13)
Operational	XPES (BL-14)
Operational	XRF- microprobe (BL-16)
Under development	SWAXS(BL-18)
Operational	Protein Crystallography (BL-21)
Operational	X-ray Beam Diagnostic (BL-23)
Operational	Visible Beam Diagnostic (BL-24)

Operational beamlines   Beamlines under commissioning   Beamlines under development

View of Experimental Hall, Indus-2

XAFS TECHNIQUE

Spectroscopic tool which provides structural information about a sample by the analysis of its x-ray absorption spectrum, *does not require long range order.*

How?: Absorption Spectrum generated using tunable bright X-ray source: Two regions

X-rays are absorbed by all matter by Photoelectric effect

XAFS is a type of diffraction pattern produced by the interference of outgoing and back scattered electron waves (in-situ LEED)

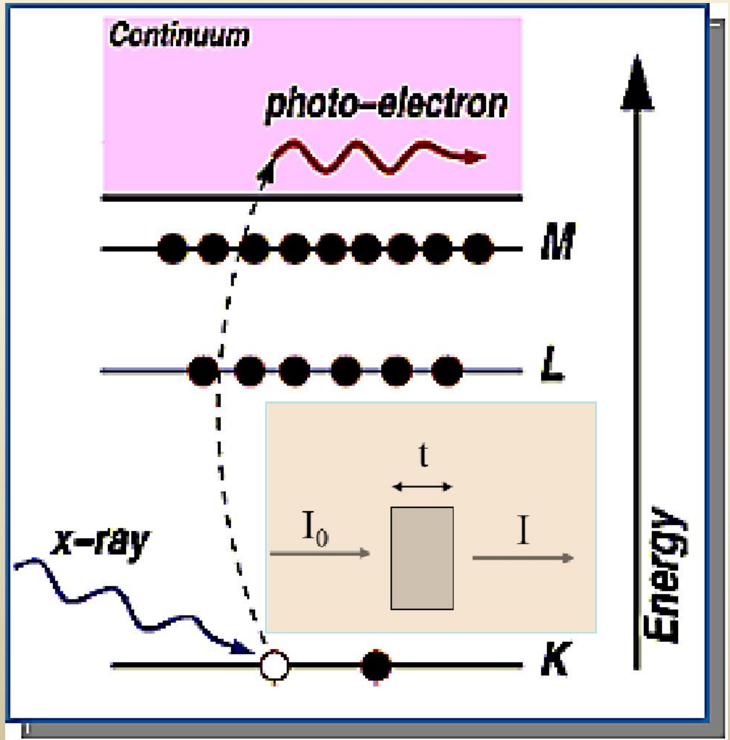

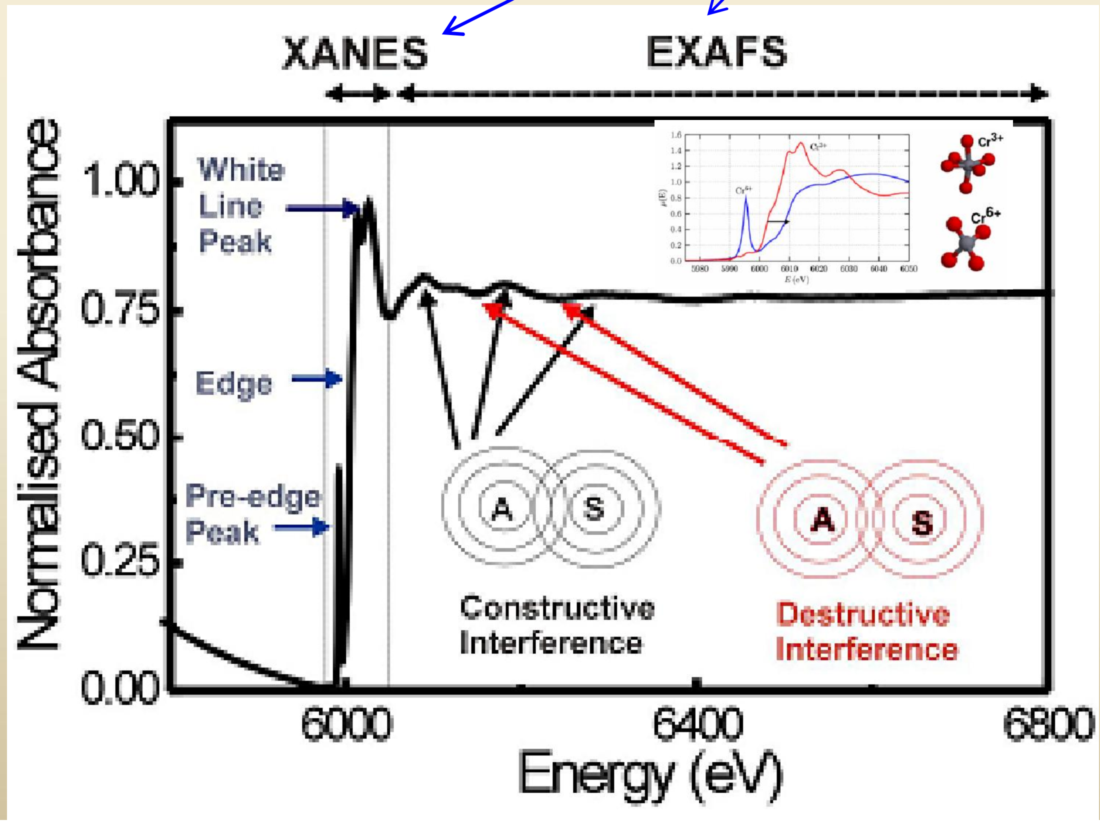

X-ray Absorption Fine structure (XAFS) Technique

Information from XAFS

XANES

- Oxidation state
- Coordination chemistry (tetrahedral, octahedral) of the absorbing atom
- Orbital occupancy

EXAFS

- Radial distribution of atoms around the photoabsorber (bond distance, number and type of neighbours)

$$\chi(k) = S_0^2 \frac{NA(k)}{kR^2} e^{\frac{-2R}{\lambda}} sin(2kR + \phi(k) + \phi_c) e^{-2k^2\sigma^2}$$

Application:

- Local structure in non-crystalline matter
- Local environment of an atomic impurity in a matrix of different atomic species
- Study of systems whose local properties differ from the average properties
- Detection of very small distortions of local structure

Powerful tool for: Magnetic materials, Materials Science (high Tc, CMR,..), Amorphous and liquid systems, Thin films and Surface Science.

Requirements of EXAFS experiment

- XAFS spectra consist of small variations in the absorption coefficient *μ(E)*
- One requires S/N ratios better than 10^3 in order to determine the spectra accurately enough in the region ≈ *600–1000 eV*
- *An intense & tunable beam is required to obtain good data in reasonable time(minutes to hours); 10^{10} photons/sec or better(SR is must)*
- *Intensity of beam should not very much during scan*
- *Energy band width should be order of 1eV to resolve EXAFS features*
- *Beam at sample should be as small as possible: microns to mm size*

Above requirements:

- impose significant demands on the design and quality of the mechanics and control system of beamline that is to be used for XAFS.
- Requirements of Beamline

Experimental station:

- wide range of sample environments [T, P, magnetic field, vacuum, “in situ”...])
- Sample should be homogeneous in thickness & particle size

Resources:

•INTRODUCTION TO XAFS A Practical Guide to X-ray Absorption Fine Structure Spectroscopy, GRANT BUNKER, *Illinois Institute of Technology, CAMBRIDGE University Press*

•X-ray Absorption: Principles, Applications, Techniques of EXAFS, SEXAFS and XANES in Chemical Analysis Vol. 92, D. C. Koningsberger and R. Prins, ed., John Wiley & sons, 1988

Experimental geometry for XAFS measurements:

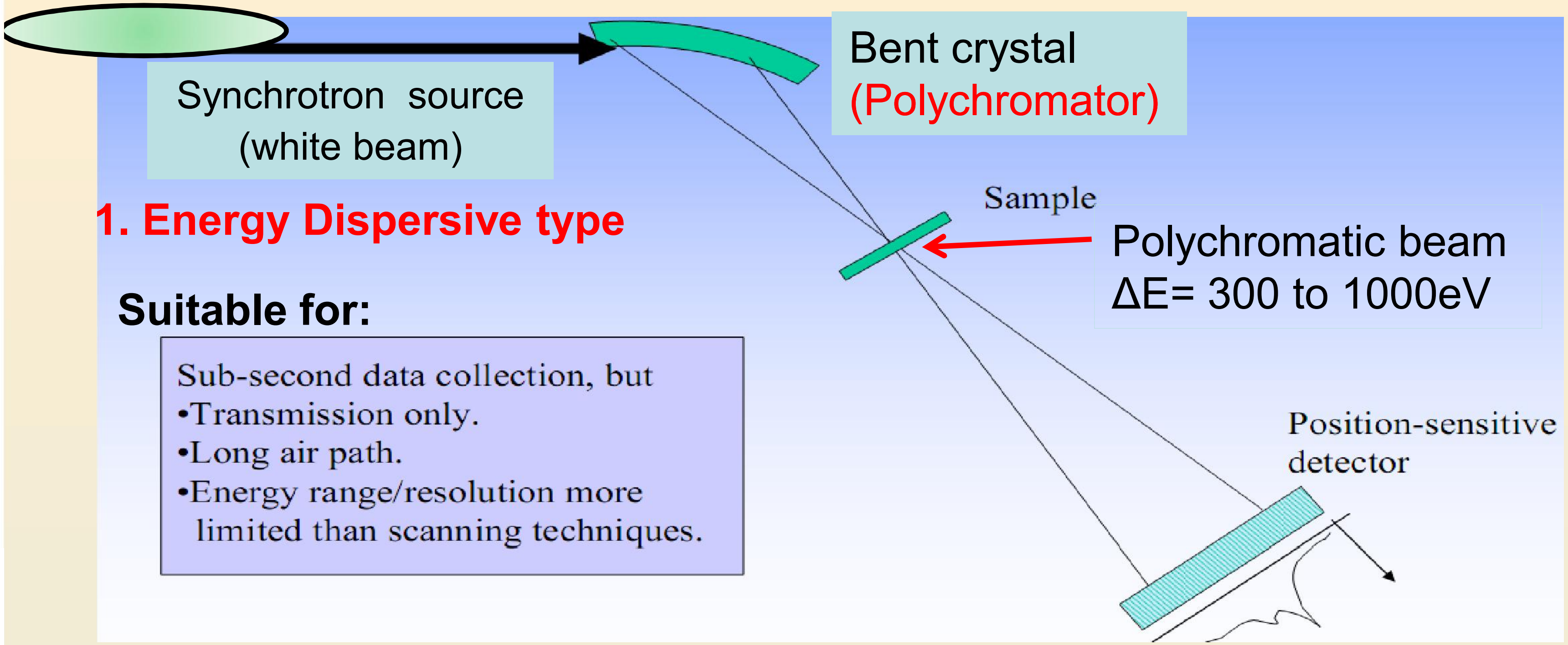

1. Energy Dispersive type

Suitable for:

Sub-second data collection, but
- Transmission only.
- Long air path.
- Energy range/resolution more limited than scanning techniques.

2. Energy Scanning type

Suitable for:

High resolution, fluorescence mode , thin film, dilute samples

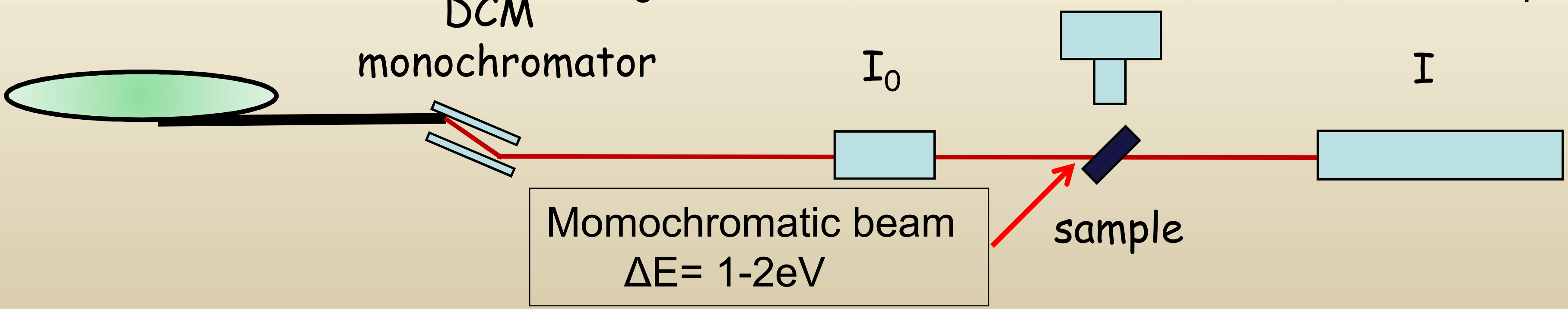

Most of the Synchrotron Radiation facilities have both Dispersive & Scanning type EXAFS Beamlines to cater the needs of wide variety of samples

XAFS Beamlines at Indus-2

- Energy Dispersive EXAFS BL(BL-08)
  - Open to users since March 2008
- Energy Scanning EXAFS BL (BL-09)
  - Open to users since Feb. 2013.

Beamlines are complex instruments , a interface between storage ring & sample that perform a variety of functions:

Safely transporting the X-rays to the experimental area; Preparing the beam for the experiment

by

precollimating,monochromating, focussing, and shuttering the beam using X-ray optics; performing precisely timed data acquisition that is synchronized to the motions of beamline optics

- K-edges of elements from

  Ti (4.966keV) **to** Mo(20000eV)
- L-edges :

  Rare earths and other high Z elements e.g W, Pb...

Characteristics of Dispersive EXAFS (BL-8) at Indus-2

- Source: Bending magnet port BL-08
- Energy range: 5-20keV
- Resolution: 10^{-4} ($\Delta E/E$)
- Band pass: 300ev to 2000eV
- Flux: 10^{12} photons/sec/1000eV
- Polychromator: Si(111)
- Detector: CCD(2k x 2k ; pixel: 13.5x13.5 μm)

Optical Layout of DEXAFS Beamline at Indus-2

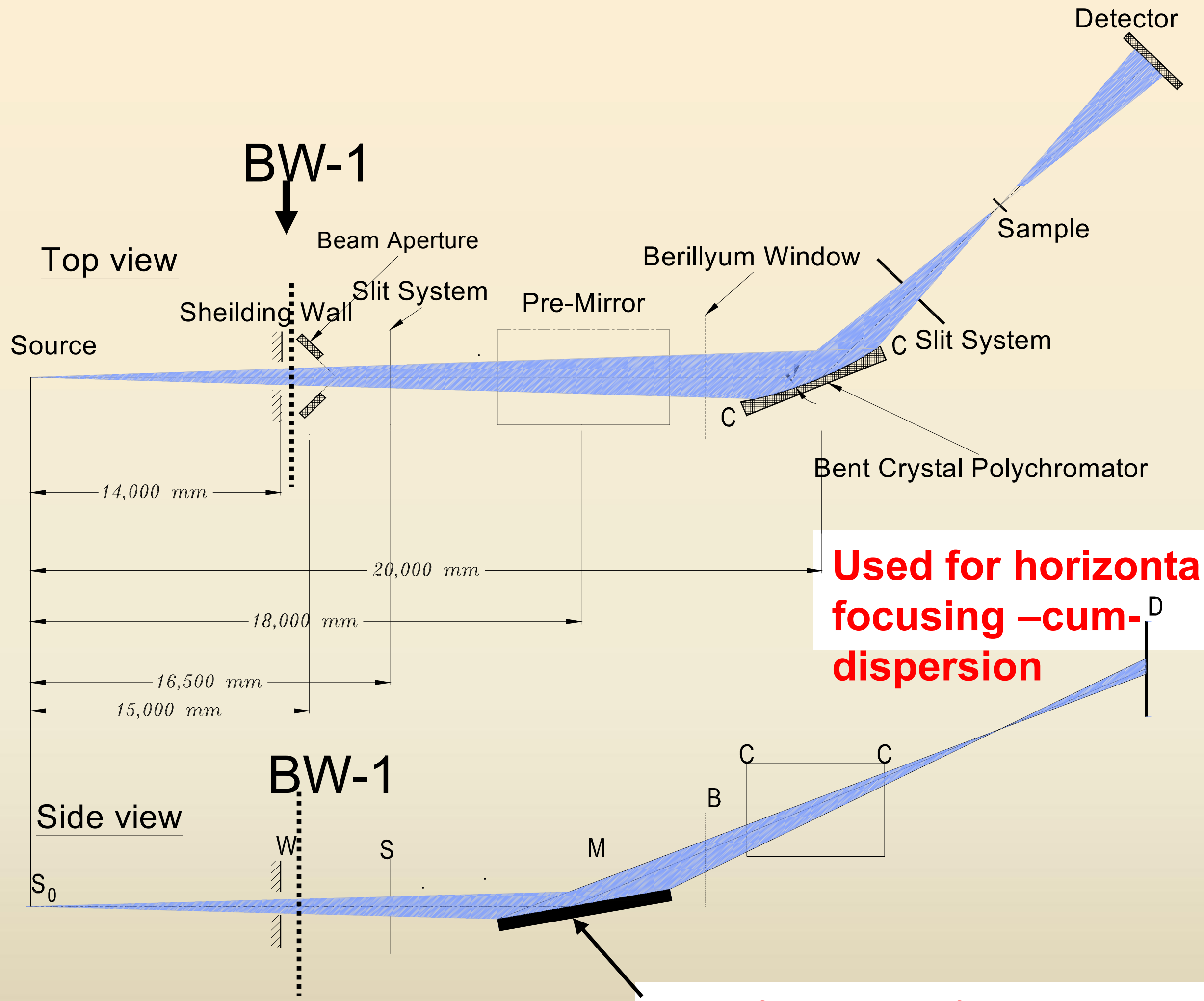

Used for horizontal focusing –cum-dispersion

Used for vertical focusing –cum-higher harmonic rejection

Ref.: N.C. Das, S.N. Jha, & D. Bhattacharyya, Proc. 8th International Conference on SRI, AIP conference proceedings, 705, 301(2003)

Beam spot measured at sample position

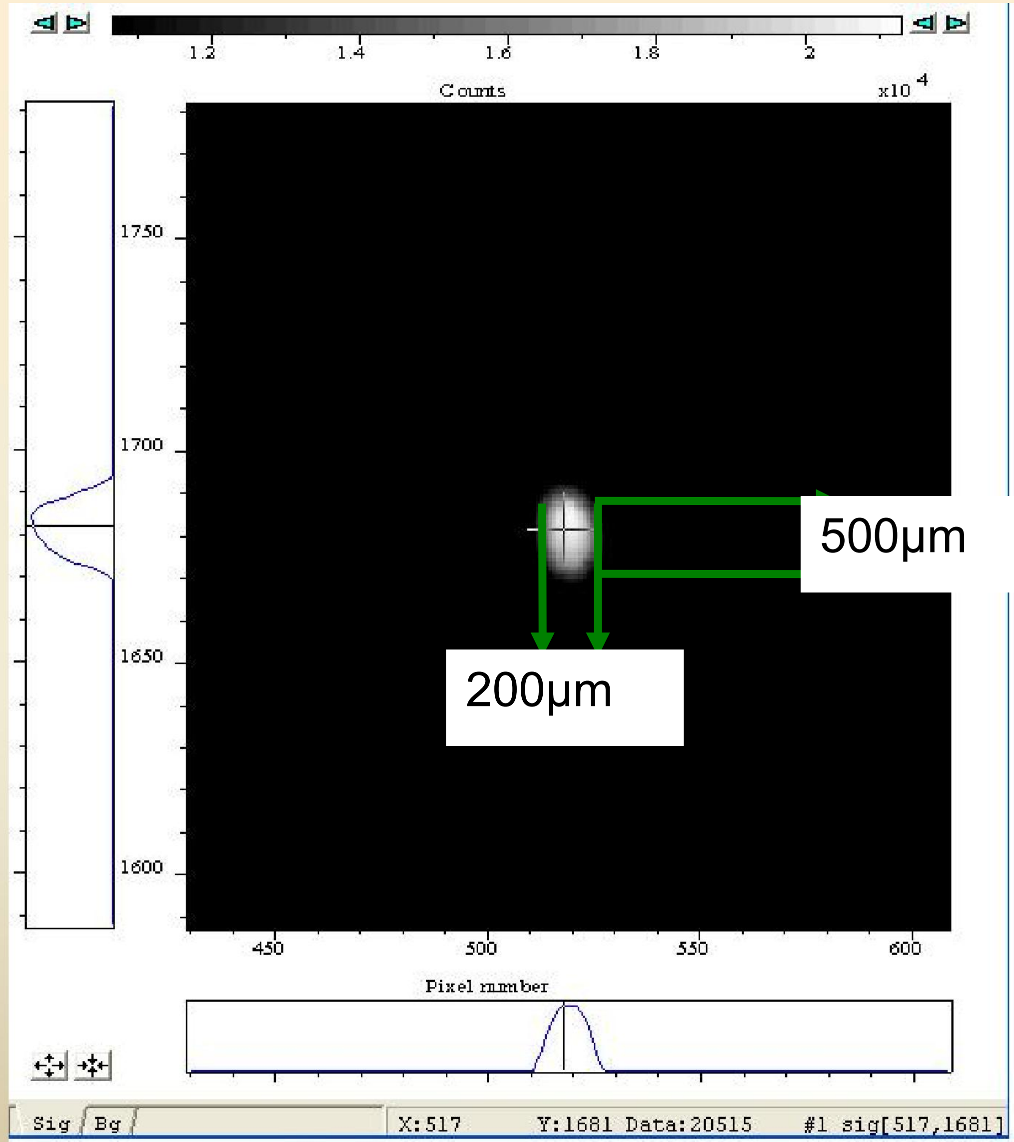

Sample size can be as small as 500microns

Experimental station

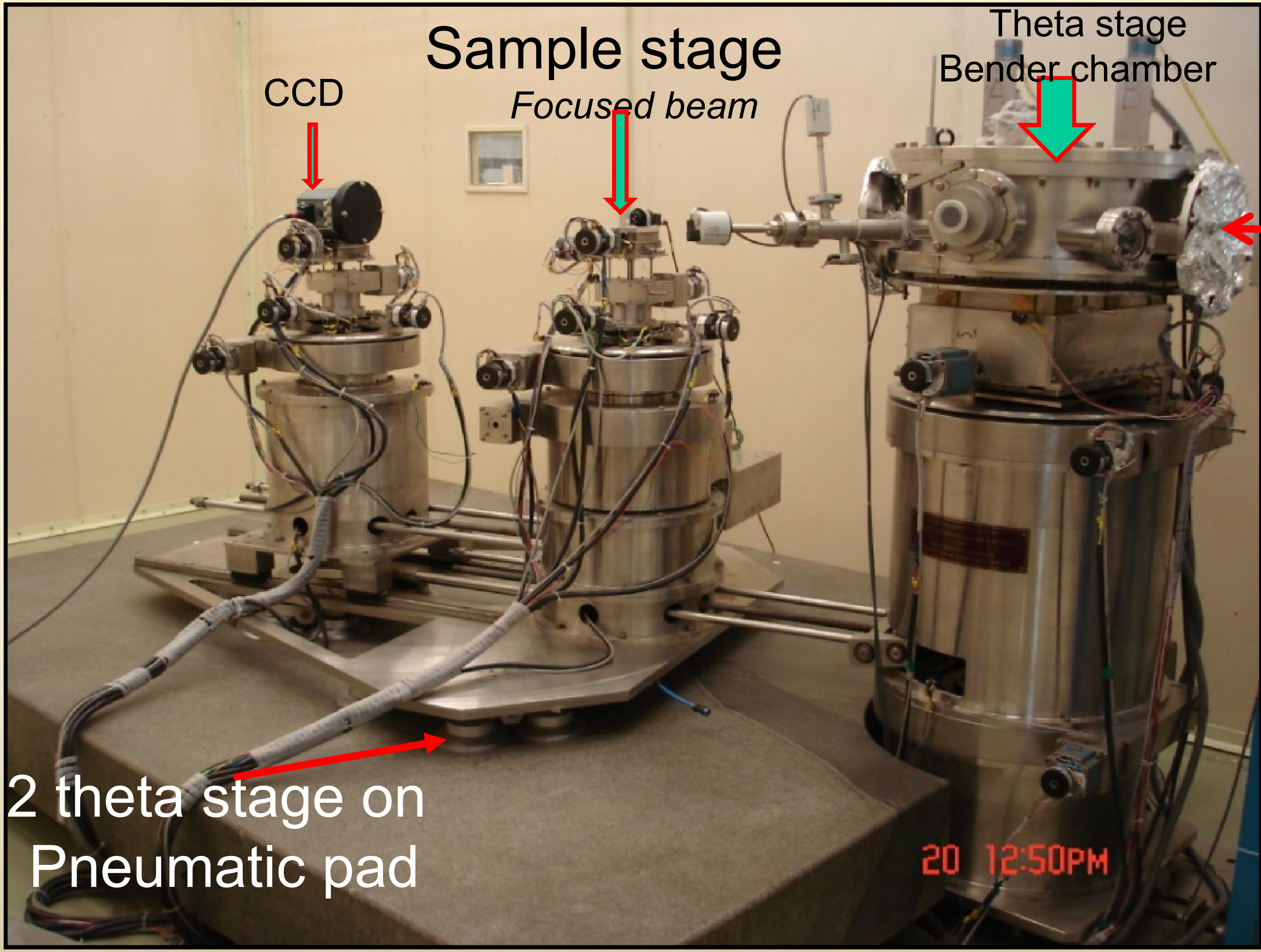

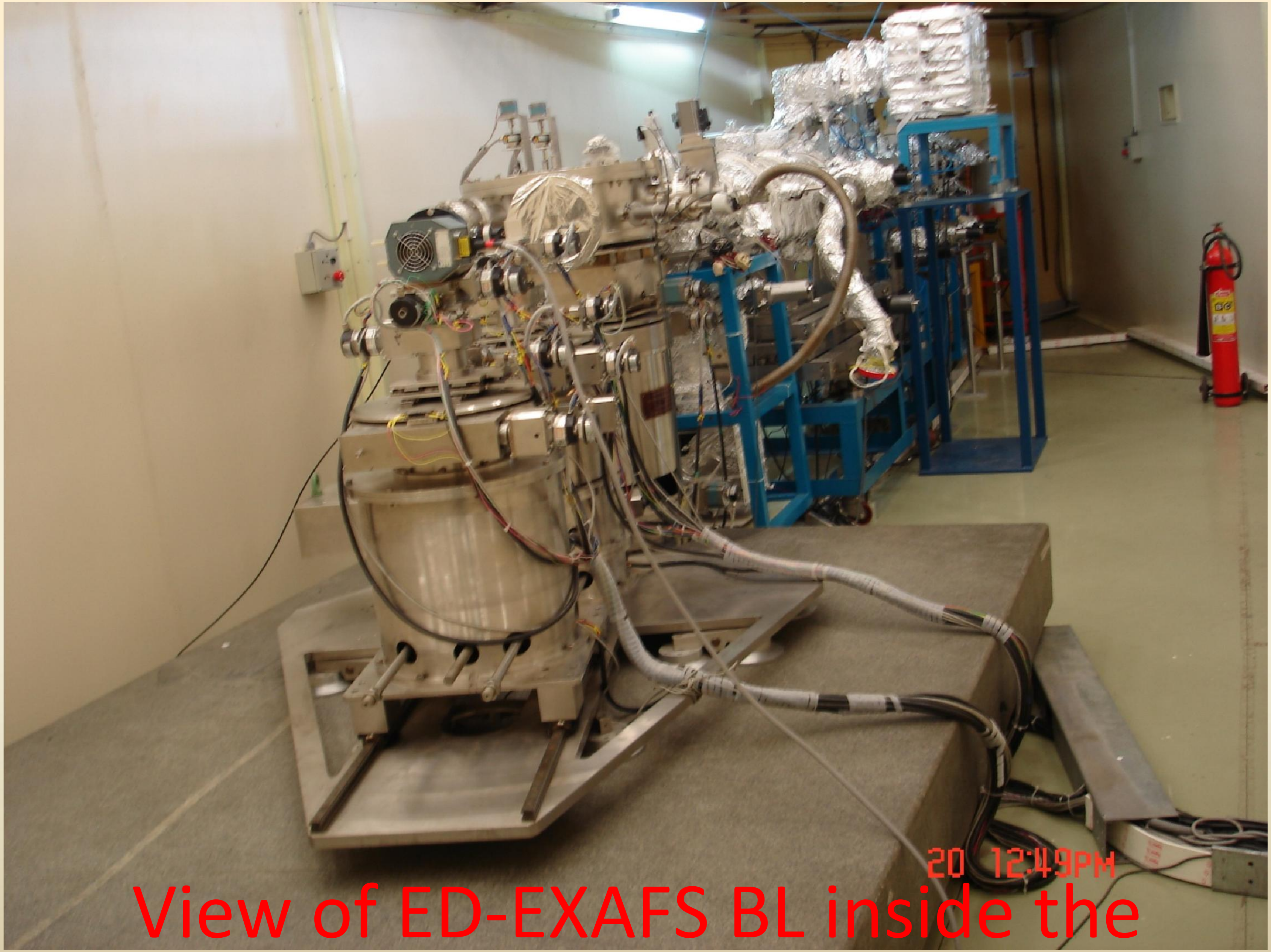

View of ED-EXAFS BL inside the hutch at Indus-2

The first result from BL-08

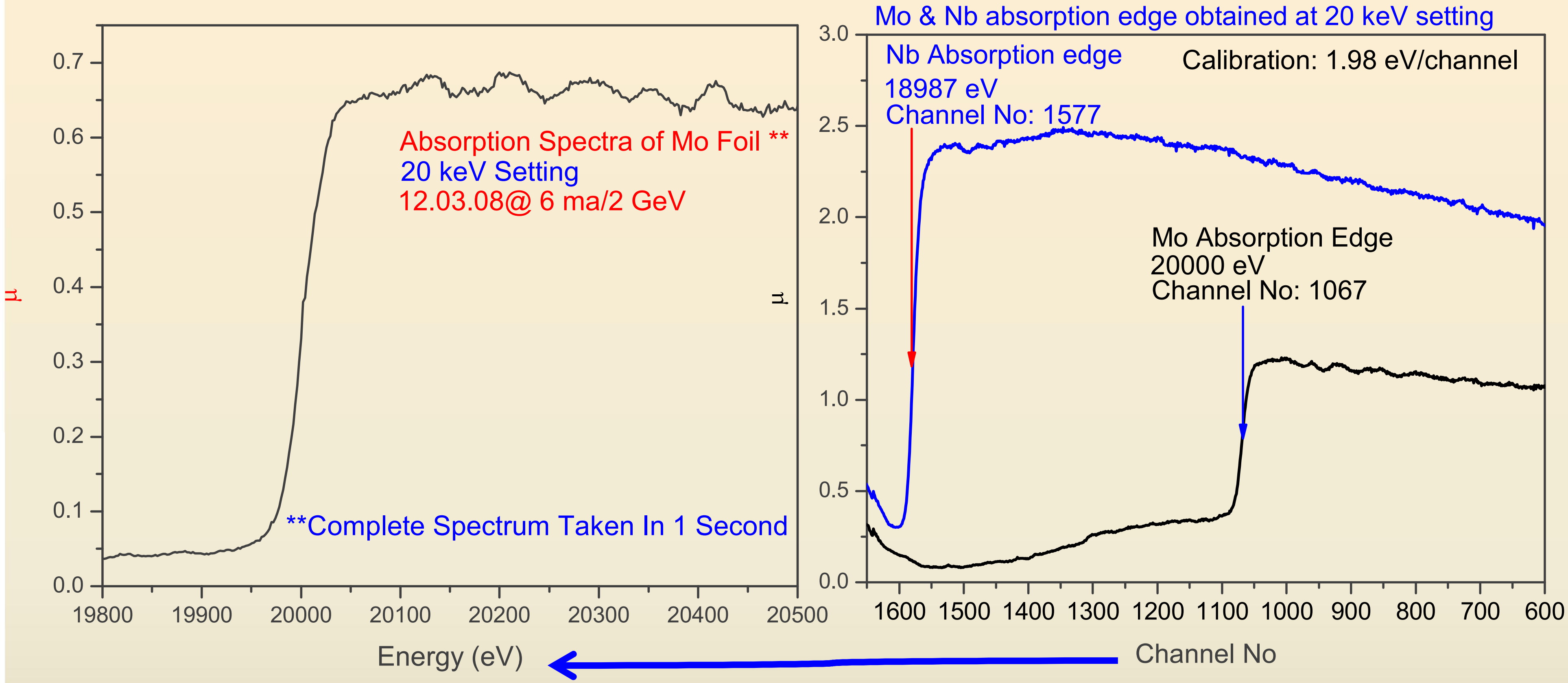

Energy	20 keV	13 keV	11 keV	7keV
Resolution	**5×10^3**	**7.5×10^3**	**8.5×10^3**	**$\sim 10^4$**

D. Bhattacharyya, A.K. Poswal, S.N. Jha, Sangeeta and S.C. Sabharwal, Nucl. Instrum, Meth. Phys. Res. A 609, 2009, 286.

A comparative study of the spectra recorded at RRCAT synchrotron BL-8 dispersive EXAFS beamline with other beamlines

ABHIJEET GAUR[a*], B. D. SHRIVASTAVA[a],

S. N. JHA[b], D. BHATTACHARYYA[b] AND A. POSWAL[b]

[a]School of Studies in Physics, Vikram University, Ujjain-452001, M.P.

[b]Applied Spectroscopy Division, Bhabha Atomic Research Centre, Mumbai-400085

* abhijeetgaur9@gmail.com

Conclusion:

The present work is a comparative study of the XAFS spectra recorded at the BL-8 beamline with those recorded at three other well known synchrotron EXAFS beamlines. For this study, two examples have been taken, one of copper metal (strong EXAFS oscillations case) and another of copper complex (weak EXAFS oscillations case). Theoretical models have been generated for both copper metal and the complex and fitted to their respective experimental EXAFS spectra to obtain the structural parameters. The structural parameters obtained by using BL-8 beamline have been found to be comparable to those obtained from other beamlines. Also, the results obtained from EXAFS data for the copper complex have been found to be comparable with the crystallographic results. Thus, it is seen that the spectra recorded at the BL-8 beamline

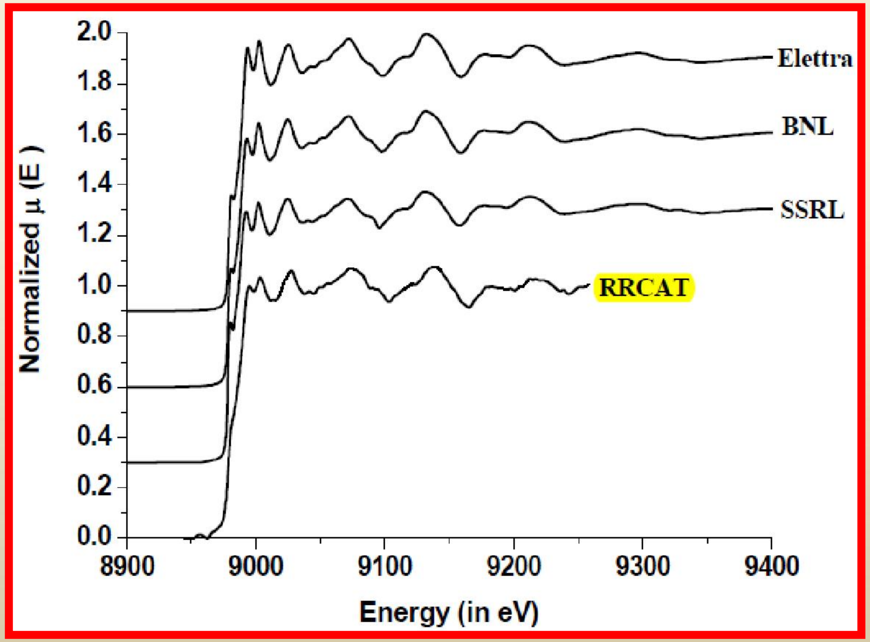

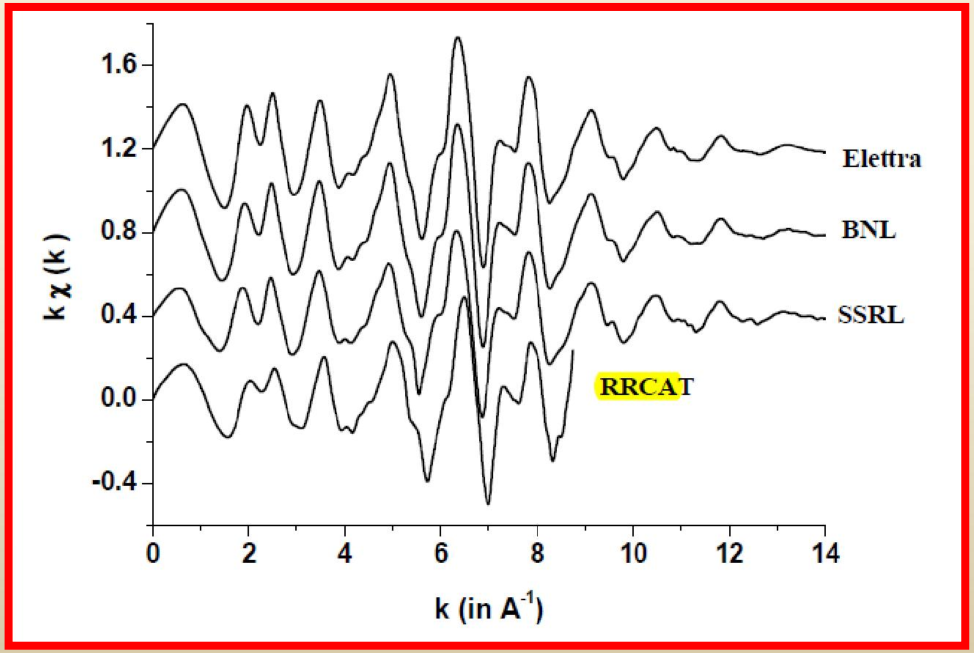

Pramana, 80 (2013) 159.

2. Energy Scanning EXAFS beamline(BL-9)

Energy Scanning Type EXAFS beamline

Source: Bending magnet

Target Specifications:

- **Energy Range: 4 keV - 25 keV**
- **Resolution (E/ΔE): 10^4**

Schematics of Optical layout of Scanning EXAFS beamline

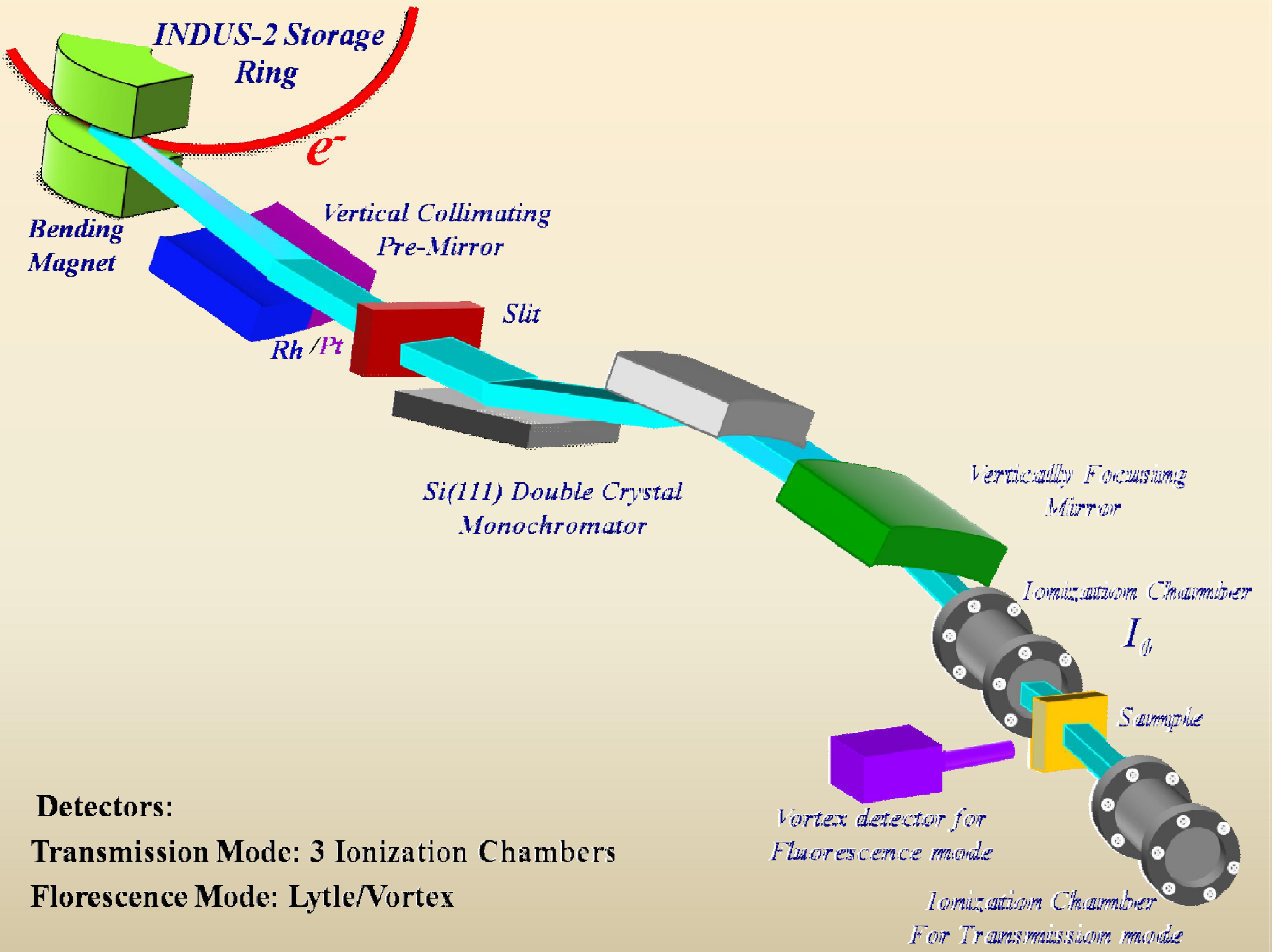

Detectors:

Transmission Mode: 3 Ionization Chambers

Florescence Mode: Lytle/Vortex

Mechanical layout of Scanning EXAFS Beamline(BL-9)

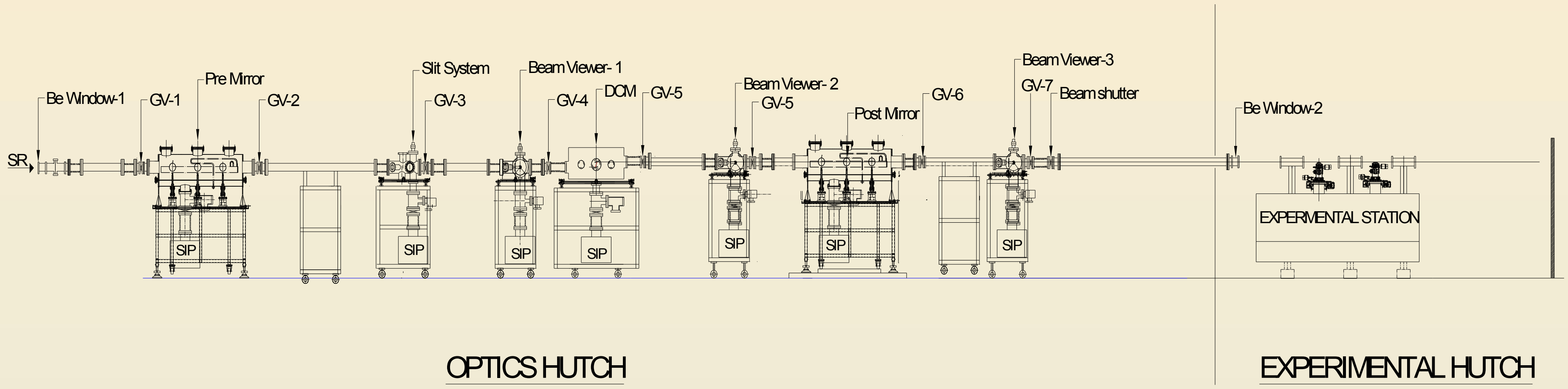

Maintained at UHV

BL length: ~37meter from source point

Scanning XAFS beamline

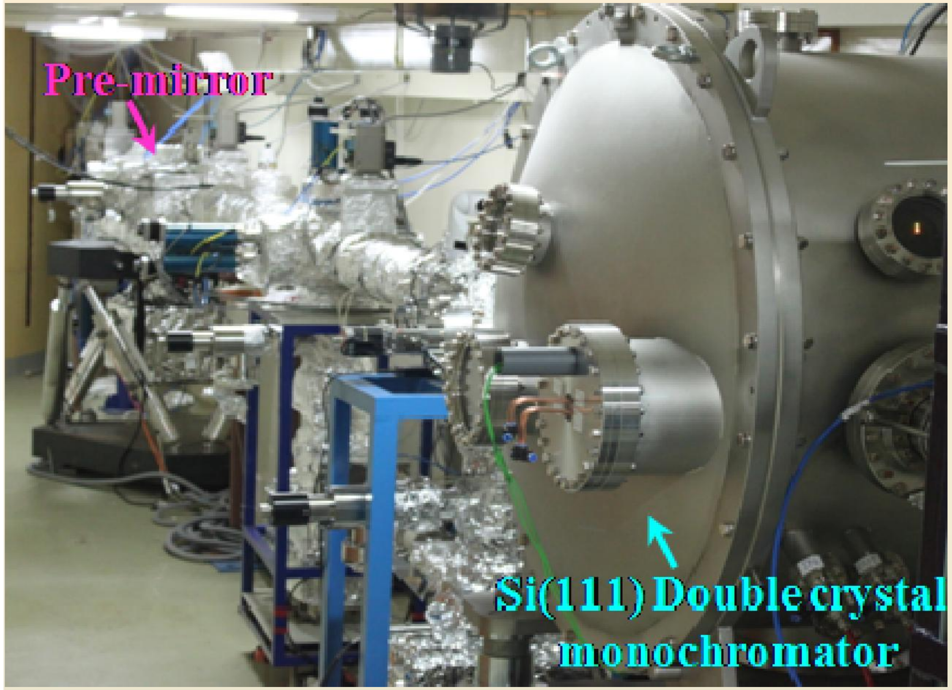

View of optics hutch

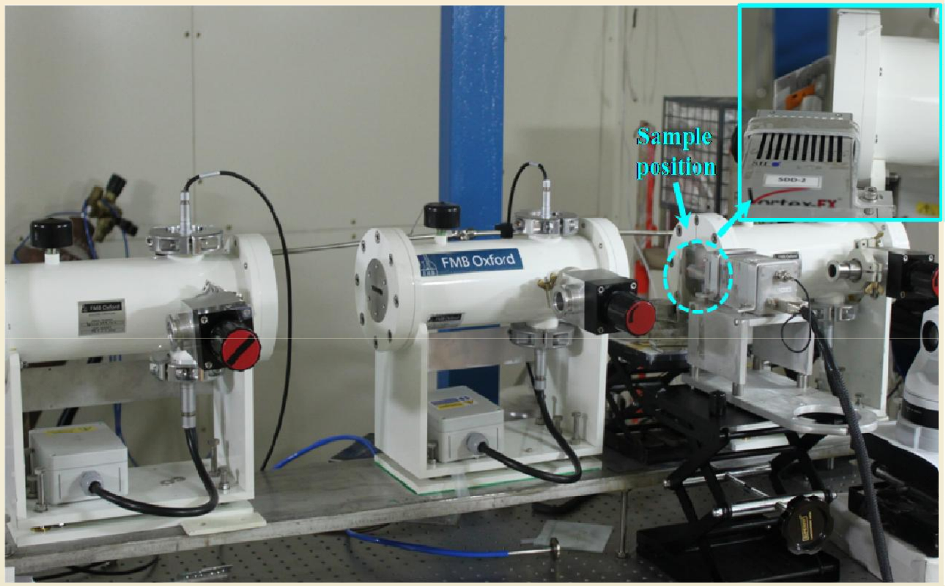

View of Experimental station

Sample environment : CCR He cryostat up to 10 K
High temperature cell upto 1000 K

Available detectors : Ionisation chambers (3 Nos) for transmission mode EXAFS
: Lytle & Vortex (SDD) Detectors for fluorescence mode

First result from BL-9

Beam at Front-end(at 16meters from source point)

Observed on 22nd Sept 2012
23:45 hrs

First absorption spectrum recorded
22nd Nov. 2012

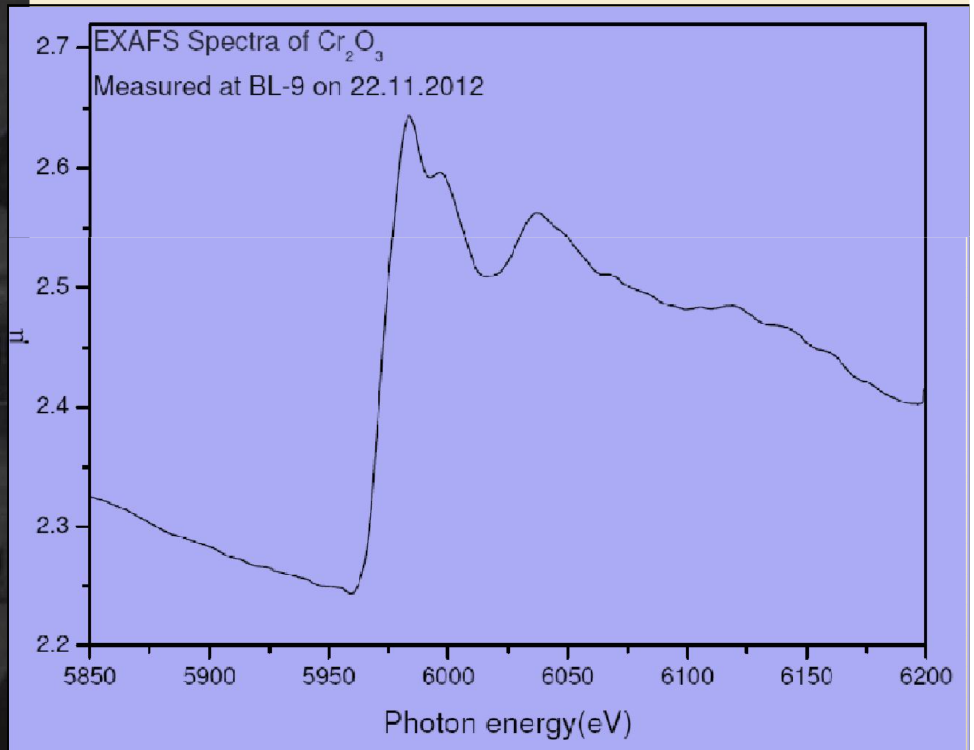

Data to illustrate the performance of Scanning EXAFS beamline

XAFS spectra of vanadium compounds in transmission mode

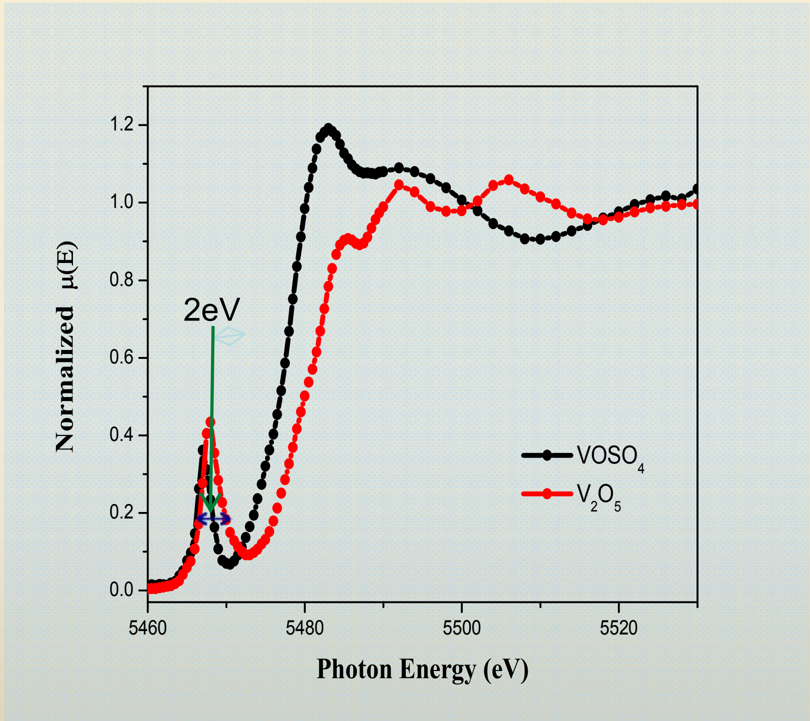

XAFS spectrum of Y_2O_3 thin film recorded in fluorescence mode

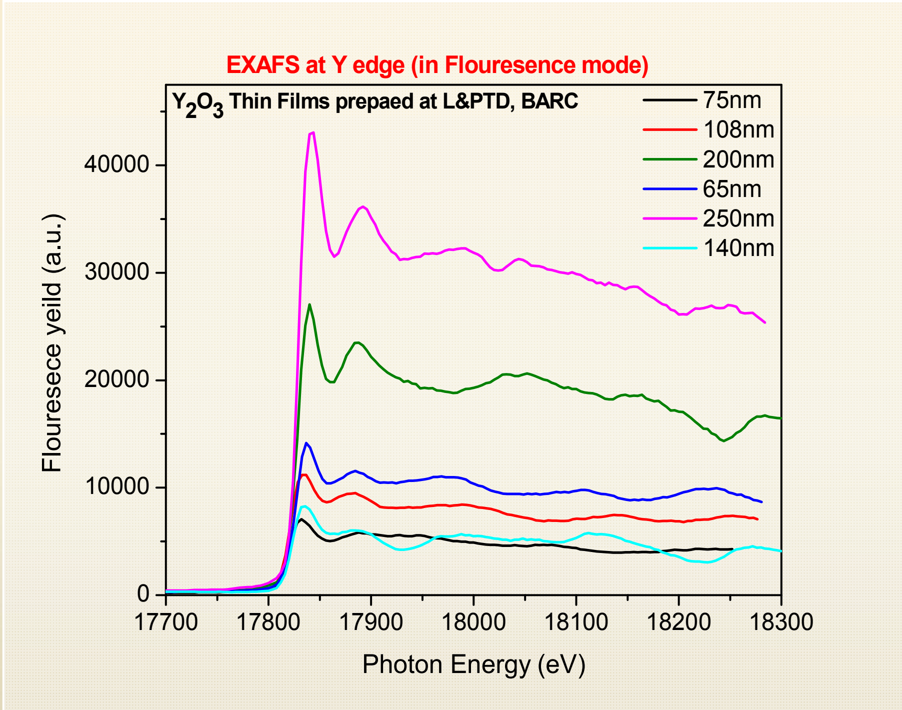

Commissioning and First Results of Scanning Type EXAFS Beamline (BL-09) at Indus-2 Synchrotron Source, A K Poswal, A Agrawal, A K Yadav, C Nayak, S Basu, S R Kane, C K Garg, D Bhattachryya, S N Jha, N K Sahoo, 58thDAE SSPS, Thapar Univ., Patiala, December 17-21, 2013.

..........Data to illustrate the performance of Scanning EXAFS beamline

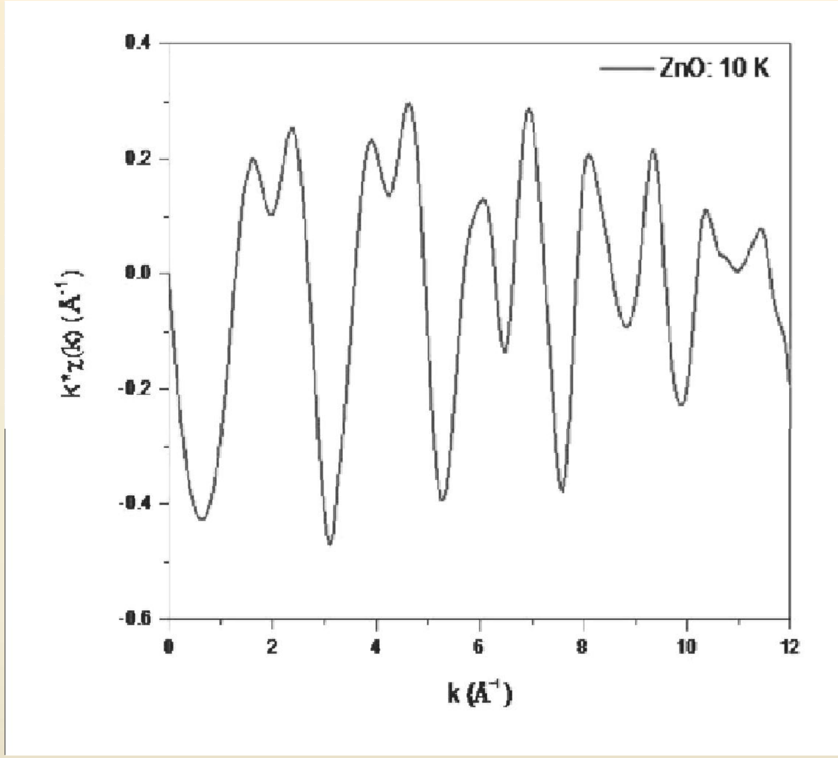

XAFS spectrum of ZnO nanomaterial recorded at 10K

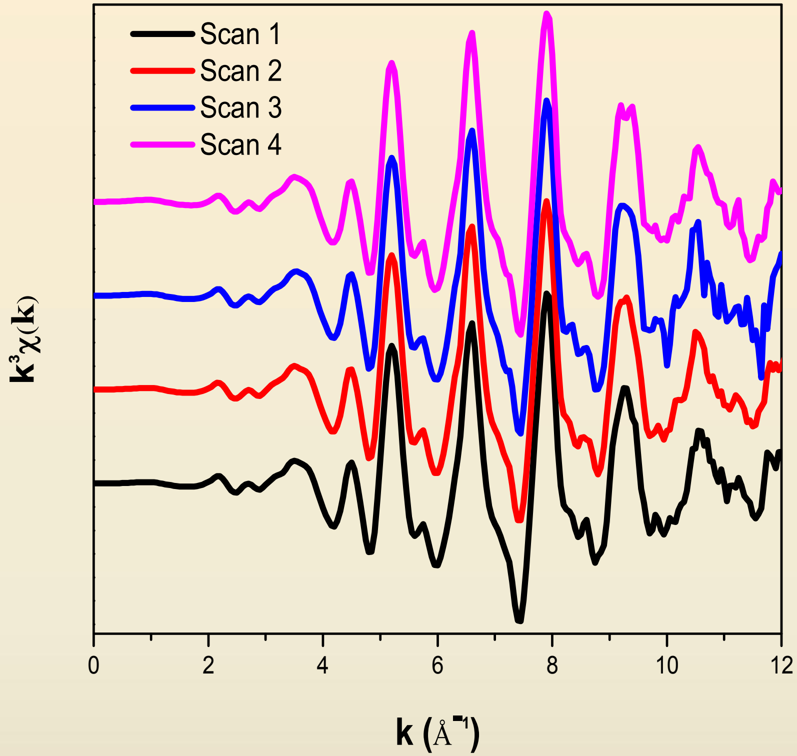

Repeated EXAFS spectra of V metal foil

Examples of studies

EXAFS studies of doped ZrO_2 systems

Samples prepared at : Chem. Div., BARC ; Applications : Intermediate temp. solid electrolytes

- **Zirconia exhibits high anionic conductivity when doped with aliovalent cations which initiates the generation of oxygen ion vacancies for charge compensation.**

- **Yttria-stabilized zirconia (YSZ) typically at 8mol% yttria, is the most common material used in Solid Oxide Fuel Cells (SOFCs).**

- **Limitation**

  Operate at relatively high temperatures of around 1100–1300K to achieve adequate ionic conduction. This has prompted the search for alternate materials with equivalent ionic conductivity at lower temperature.

Measurements were done on two sets of samples at the Zr K-edge, viz., (i) Zirconia doped with 11 mol% of Gd^{3+}, Nd^{3+}, La^{3+}, where the dopant cations are in the order of increasing ionic radii and (ii) zirconia doped with 7, 9, 11 and 13 mol% of Gd.

- **Aim of the study**

To have insight into the mechanism of creation of oxygen vacancies and on their locations within the ZrO_2 matrix as a function of dopant ion size and Gd doping concentration, as there are contradictory information in the literature regarding the same.

Variation of dopant cation size:

- for larger size dopants (viz., Nd and La) the oxygen vacancies are created near the dopant site leaving the host sites unperturbed

- for smaller size dopant viz., Gd, oxygen vacancies are created near the host Zr site.

- Zr-Zr coordination also confirms that with increase in the size of the dopant cation the disorder near the host Zr cation is decreased.

- The above conclusion has been confirmed by ab-initio calculations for La-doped ZrO_2 systems .
  (Acknowledgement : Dr. Aparna Chakrabarti, RRCAT, Indore)

- Since the Gd-doped samples have the minimum oxygen coordination, it can be concluded that Gd is most effective in generating oxygen vacancies.

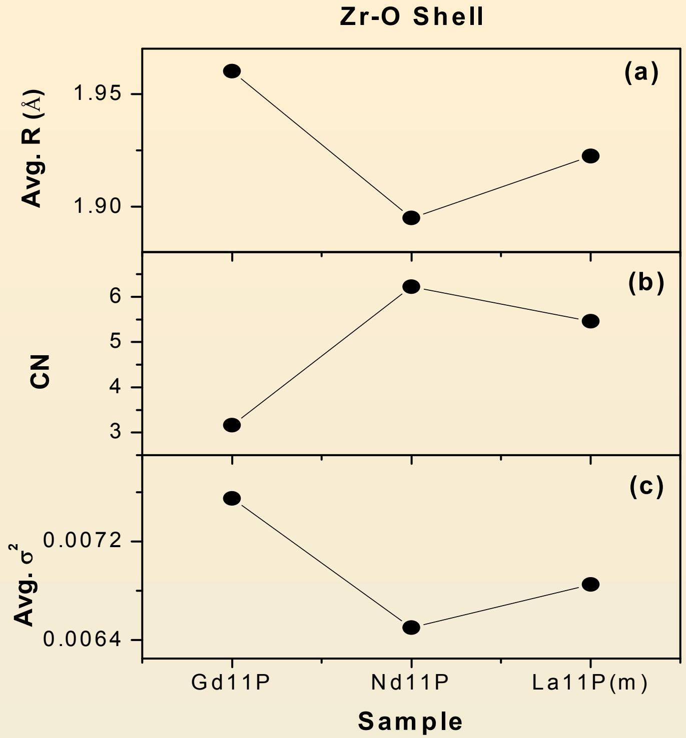

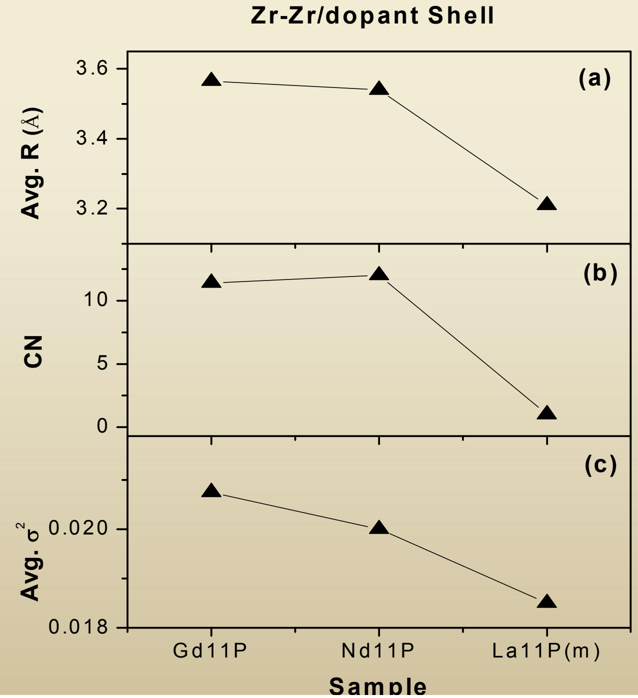

Variation in Gd concentration:

- **With increase in Gd concentration from 7% to 13%, the total oxygen coordination deceases significantly up to a doping level of 13% above which the oxygen coodination increases possibly due to clustering of Gd ions inside ZrO_2 lattice.**

Later verified by Gd-edge EXAFS measurements

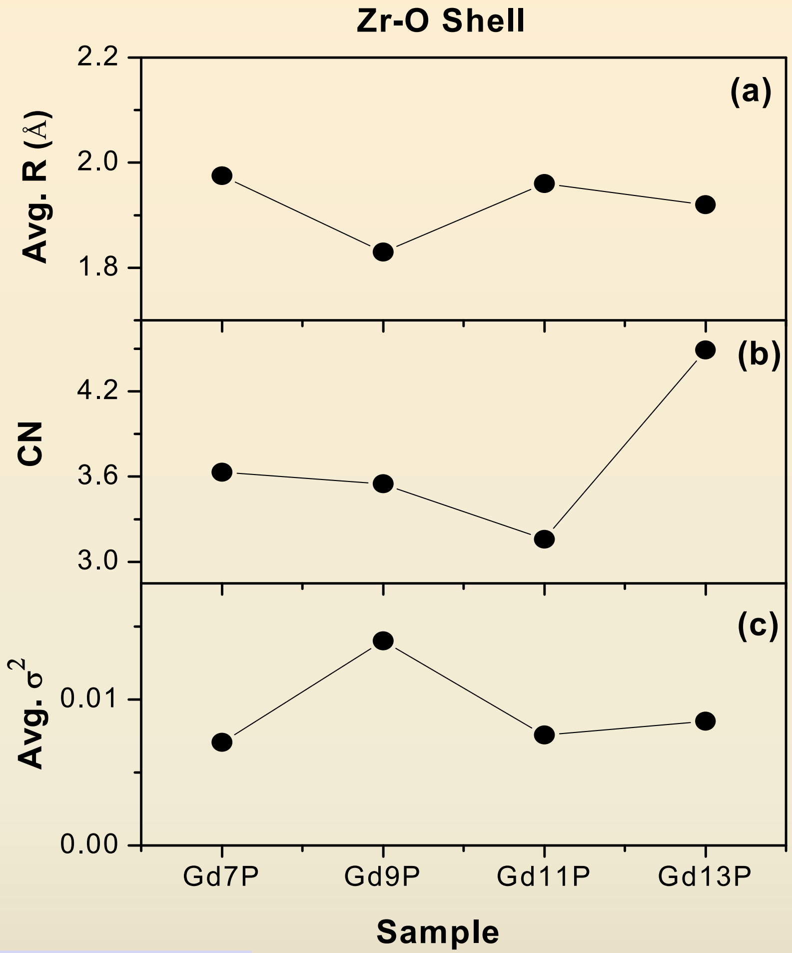

9-11% Gd doping is optimum for creation of vacancies near the Zr sites and hence for increasing its ionic conductivity

S. Basu, Salil Varma, A. N. Shirsat, B.N. Wani, S. R. Bharadwaj, A. Chakrabarti, S.N. Jha and D. Bhattacharyya, Journal of Applied Physics, 111 (2012) 053532.

Structural collapse of layered GaOOH nanorods by Eu ions

Samples prepared at : Chem. Div. BARC

- Used for the synthesis of Gallium oxide based luminescent materials and devices.
- To study changes in local environment around Ga in GaOOH nanorods brought about by the presence of lanthanide ions during its synthesis.

Measurements carried out at Ga K-edge on GaOOH : Eu (x%) x = 0, 0.5, 0.75, 1.0 & 3.0

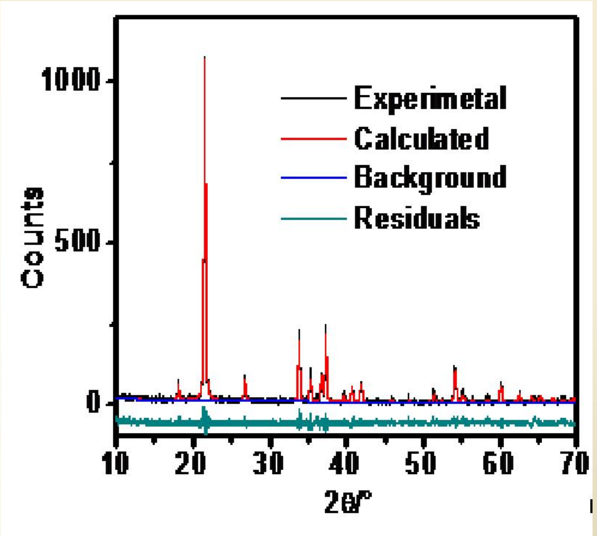

XRD pattern of Undoped GaOOH

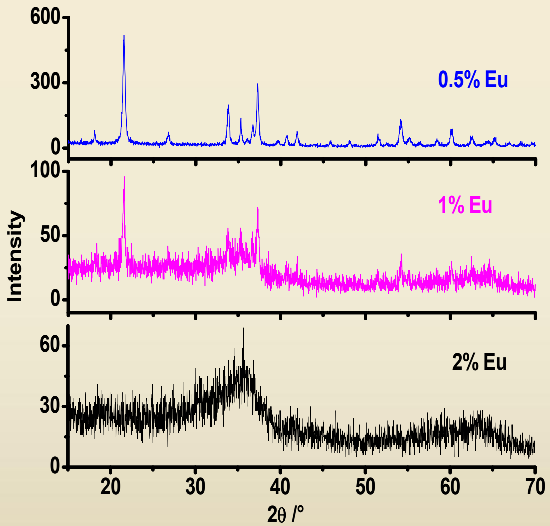

Gradual long range breakdown starting @ 1% Eu doping

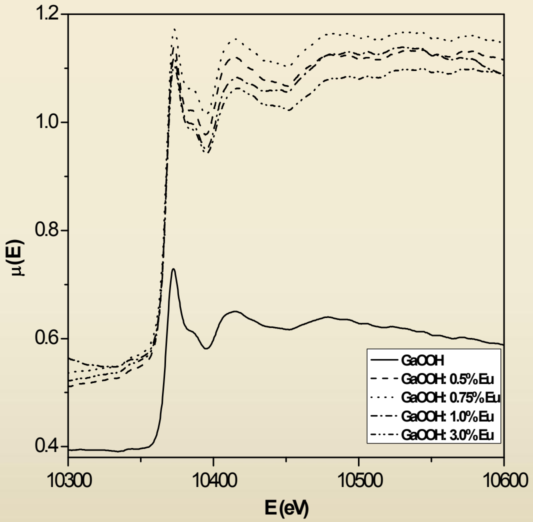

EXAFS spectra do not show any local structure distortion **But disorder increases**

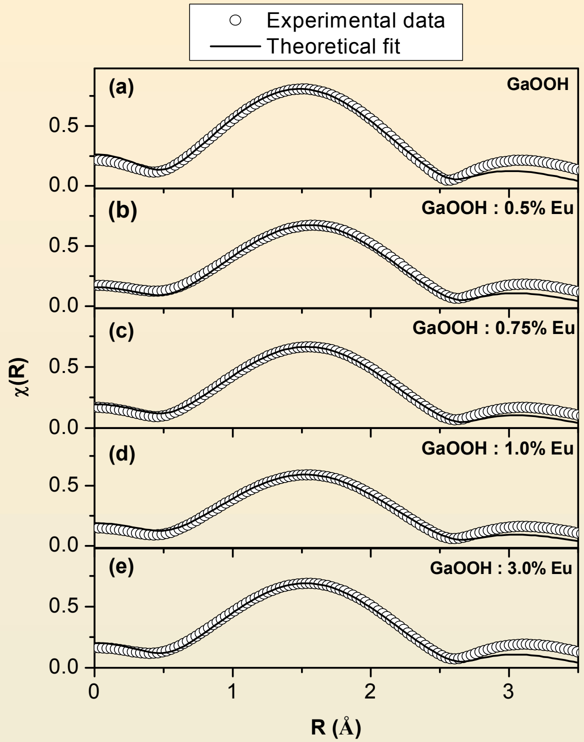

There is no change in Ga-O bond length. **Eu^{3+} do not replace Ga^{3+} as such**

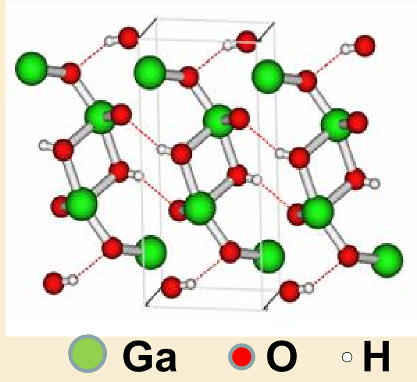

However, the disorder increases appreciably even with the introduction of a small amount of Eu^{3+} (0.5%) and reaches a maximum for 1% Eu doping

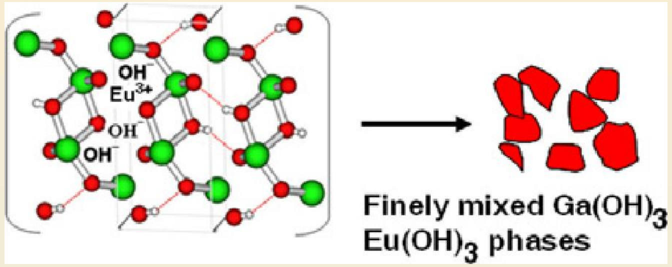

- ✓ **Eu^{3+} ions/species get incorporated at the inter-layers of GaOOH wherein it preferentially interacts with OH groups to form $Eu(OH)_3$ species.**
- ✓ **Formation of such hydroxide species destabilizes the layered structure of GaOOH.**

		GaOOH	0.5Eu	0.75Eu	1.0Eu	3.0Eu
Ga-O1 (1.852 Å; 3)	R1	2.05	2.08	2.07	2.06	2.06
	N1	3	3	3	3	3
	σ_1^2	0.0077	0.012	0.0135	0.017	0.011
Ga-O2 (1.975 Å; 3)	R2	2.18	2.22	2.20	2.19	2.20
	N2	3	3	3	3	3
	σ_2^2	0.006	0.0084	0.006	0.0081	0.005
Ga-H (2.513 Å; 3)	R3	2.51	2.51	2.51	2.51	2.51
	N3	3	3	3	3	3
	σ_3^2	0.003	0.003	0.003	0.003	0.003

S. Basu, B. S. Naidu, M. Pandey, V. Sudarsan, S. N. Jha, D. Bhattacharyya, R. K.Vatsa, and R. J. Kshirsagar Chem. Phys. Lett., 528 (2012) 21.

Low temperature X-ray Absorption Spectroscopy Study of $GaFeO_3$

(In collaboration with Das et. al. SSPD, BARC)

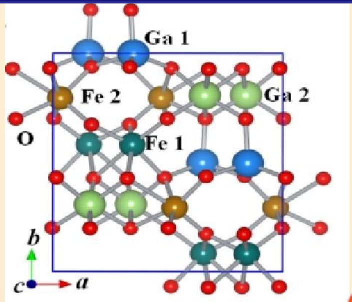

- **$GaFeO_3$ is a multiferroic system : demonstrates piezoelectricity and ferrimagnetism.**
- **Orthorhombic structure with two Ga sites (tetrahedral and octahedral) and two Fe sites(both octahedral)**
- **Ferrimagnetism occurs due to cationic site disorder and magnetic transition temperature is 200K**
- **No structural change has been observed at magnetic transition temperature from XRD/Neutron Diffraction.**

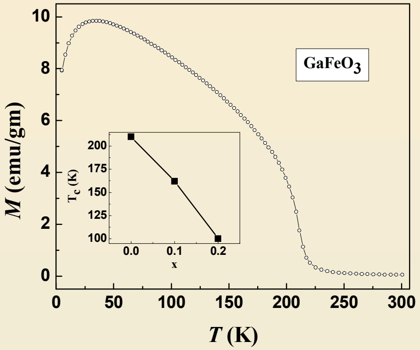

Cryostat mounted on stand at BL-09

μ versus E graphs for $GaFeO_3$

Ga K-edge

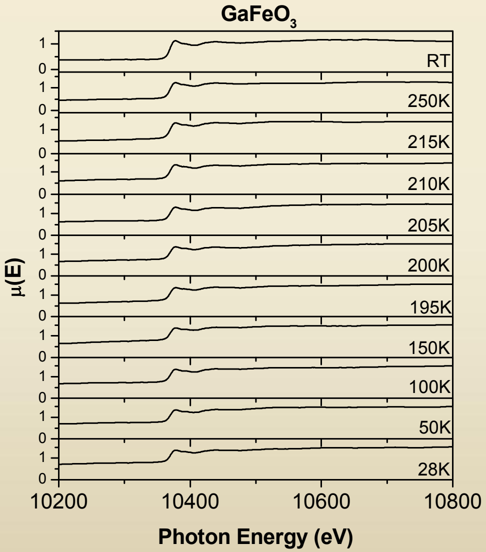

Fe K-edge

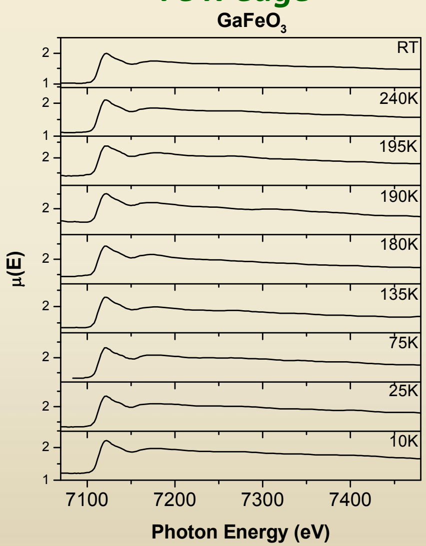

Variation of bond lengths with temperature

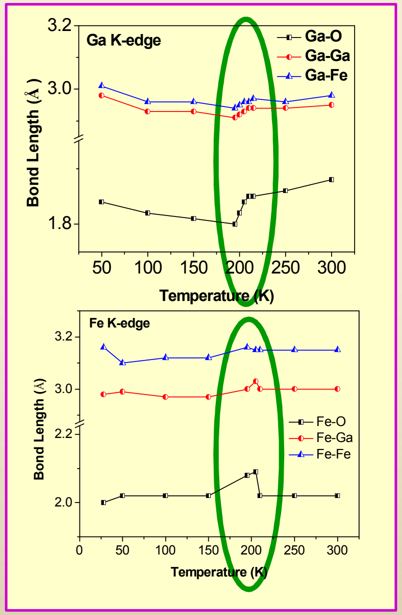

***There is clear signature of change in bond lengths at the magnetic transition temperature of 200 K**

EXAFS measurements clearly establishes the fact that magnetic transition in GFO system is related to cationic site disorder i.e. higher occupancy of Fe atoms in octahedral Ga sites.

Cu-based catalyst attached to mesoporous silica

Samples prepared at IACS, Kolkata

A **new Cu-grafted mesoporous material has been designed, which works as a heterogenous catalyst for converting** *different aryl halides with thiourea and benzyl bromide to produce aryl thioethers*.

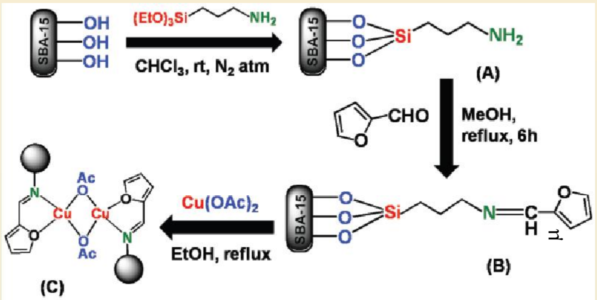

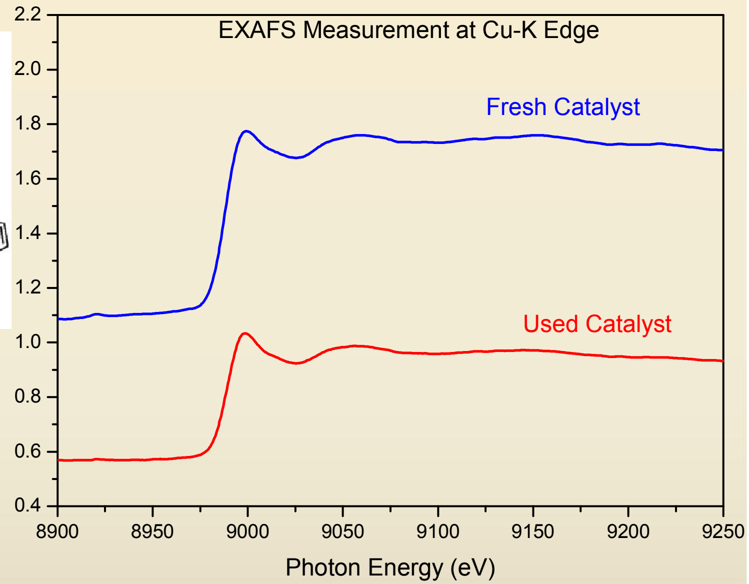

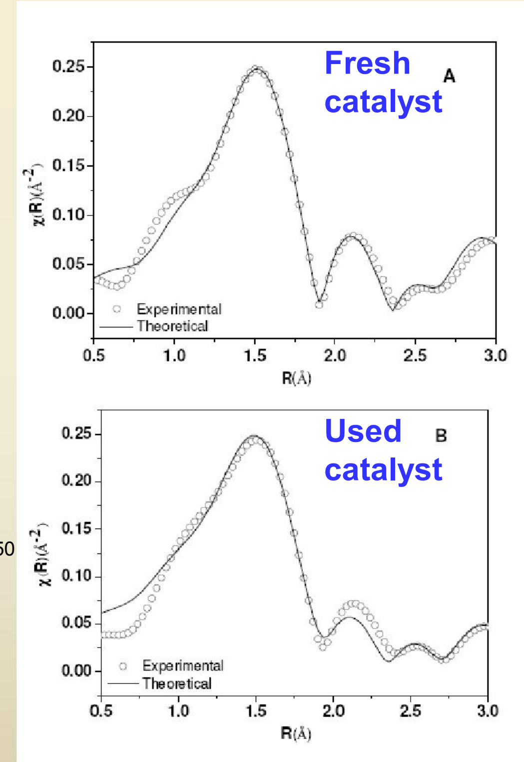

❖**EXAFS measurements has unambiguously established that local structures around Cu atom in the reused catalyst remain unchanged after the catalytic reaction.**

John Mondal, Arindam Modak, Arghya Dutta, Sohini Basu, S. N. Jha, Dibyendu Bhattacharyya and Asim Bhaumik, *Chem. Commun. 48 (2012) 8000.*

EXAFS to probe the Unexpected Adsorption-Coupled Reduction of U(VI) to U(V) and U(IV) on Borassus flabellifer-Based Adsorbents

Sample prepared: P. S. Padmaja et al. , M. S. University of Baroda, Vadodara.

➢ **Palm shell based absorbents (Biomaterial) prepared under different thermochemical condition is tested for their potential In absorption of uranium and absorption mechanism is understood using EXAFS technique.**

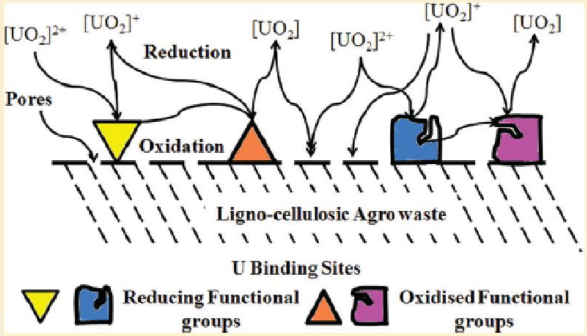

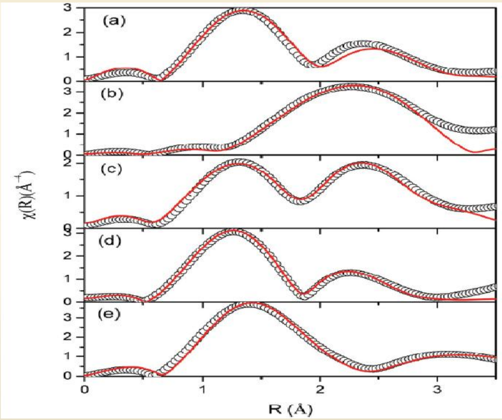

Fourier transform of ULIII-edge EXAFS for the samples (a) APSP (b) SAPSP (c) PAPSP (d) 9AAC (e) MPSP .

❖ **Normalized XANES spectra of different samples with standards UO_2CO_3 and UF_4 samples indicate that uranium may simultaneously be present in different oxidation states.**

❖ **U-O axial and equatorial bond length found by EXAFS analysis are in good agreement with the XANES prediction.**

❖ **Fourier transforms show that the intensities of the first and second shell peaks, a function of coordination number and Debye-Waller factor vary for different samples which suggests the presence of mixed uranium species.**

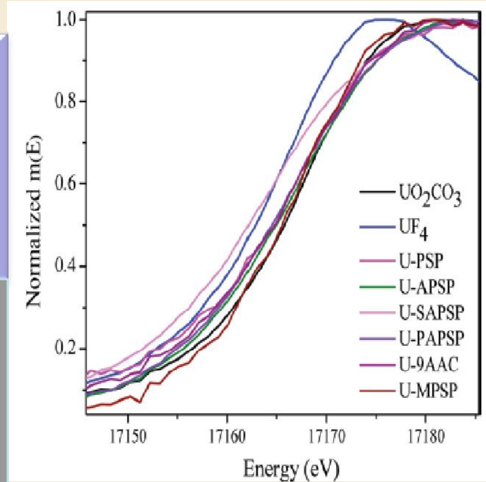

Normalized XANES spectra of different samples.

Shilpi Kushwaha, Bojja Sreedhar and P. Sudhakar Padmaja, Langmuir 28(2012) 16038.

In-situ EXAFS study of ZnO nanoparticles in different gaseous environments

Size and shape dependent structural parameters of ZnO nanostructures have been investigated under different ambience of gases.

Applications : Gas sensors

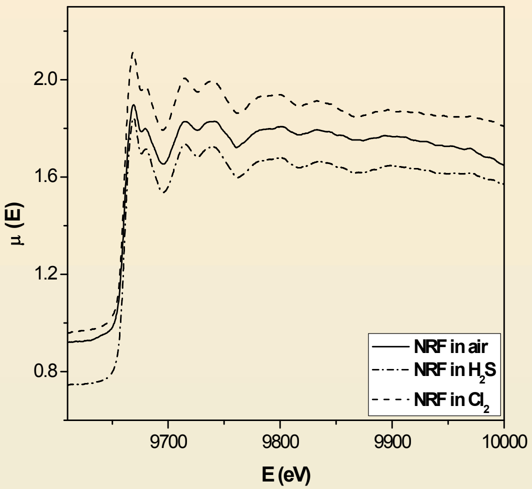

μ(E) vs E spectra of ZnO samples

This study aims at understanding the mechanism of absorption or desorption of gases in the nanocrystalline ZnO samples

Samples with particle sizes varying from 5-100 nm were investigated at the Zn K-edge (9659 eV) in air, chlorine and hydrogen sulphide atmospheres.

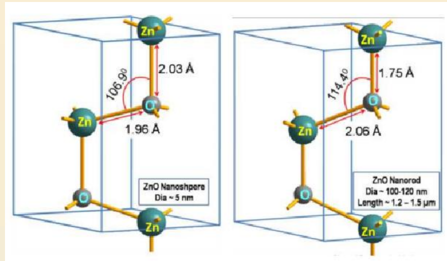

In situ reaction cell (developed in collaboration with CDM and Chem. Div., BARC)

The theoretical model assumed for fitting has 3 O atoms at 1.98 Å, 1 O atom at 1.99 Å and 6 Zn atoms at 3.21 Å

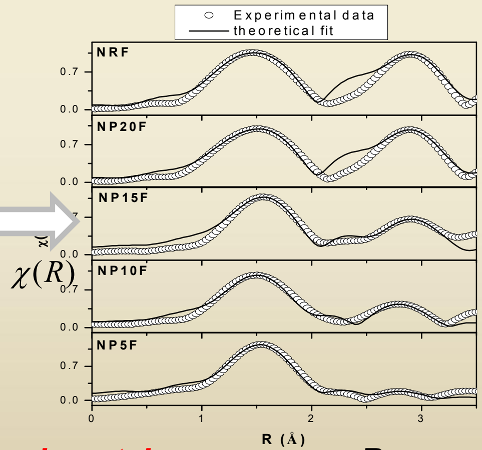

The experimental $\chi(R)$ versus R spectra and the theoretical fits of the ZnO samples in air

Manoranjan Ghosh, Dejani Karmakar,S.C. Gadkari, S.K.Gupta, S. Basu, S.N. Jha,and D. Bhattacharyya,
J. Phy. & Chem. of Solid, 75 (2014) 543.

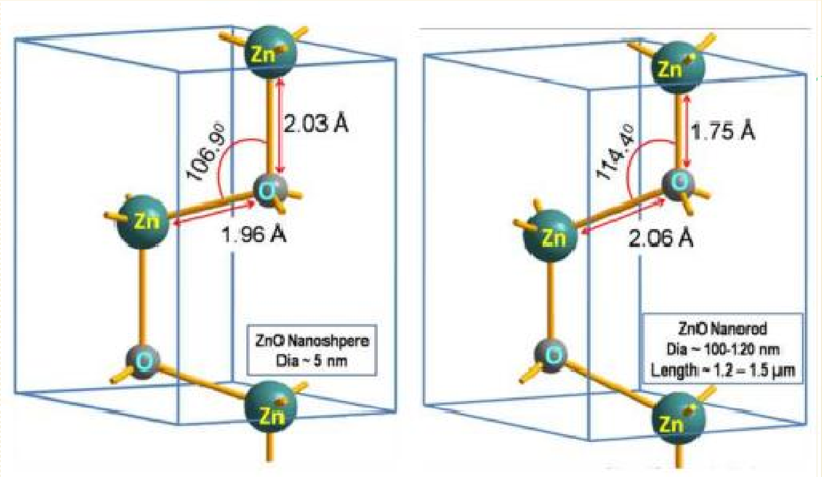

- ✓ **As the particle size decreases Zn-O bond lengths slightly increase in case of air-exposed sample giving an average value of the bulk and surface Zn-O bonds.**

In Cl_2 atmosphere, Zn-O bond length slightly decreases possibly because O vacancies in the surface are filled up by Cl atoms.

For samples treated under H_2S atmosphere, on the other hand, Zn-O bond lengths do not show any change with decrease in particle size.

- ✓ **With particle size 20 nm and below the bond length and coordination number of the Zn-Zn shell decrease and the Debye-Waller factor increases significantly.**

This implies drastic break down of the ZnO structure with reduced particle size below 20 nm.

Manoranjan Ghosh, Dejani Karmakar,S.C. Gadkari, S.K.Gupta, S. Basu, S.N. Jha,and D. Bhattacharyya, J. Phy. & Chem. of Solid, 75 (2014) 543.

Investigation into variations in local cationic environment in layered oxide series InGaO3(ZnO)m (m=1-4)

- **Layered oxides have distinct structure and electronic properties.**
- **Transparent conducting oxides combine both electrical conductivity and optical transparency in single material.**
- **Useful in solar cells, flat panel displays etc**

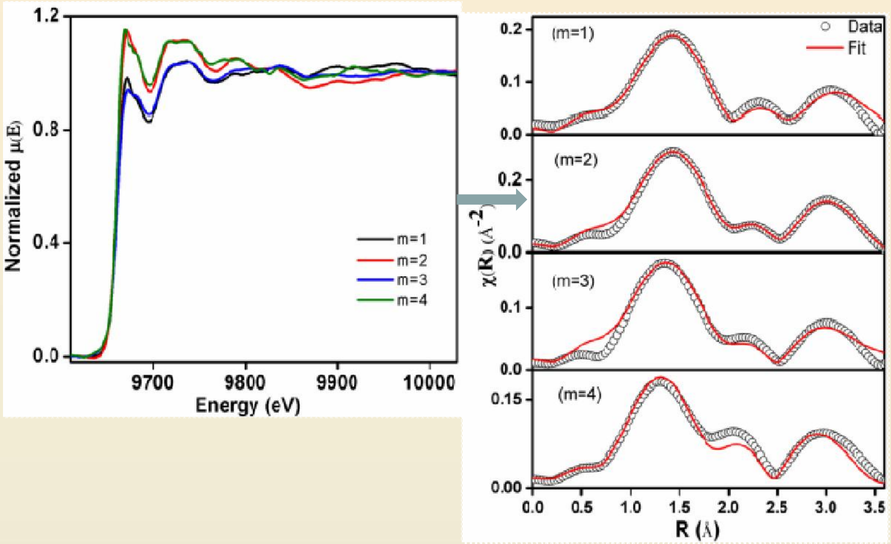

EXAFS spectra for $InGaO_3(ZnO)_m$ at Zn K-edge, & Fourier transformed EXAFS spectra

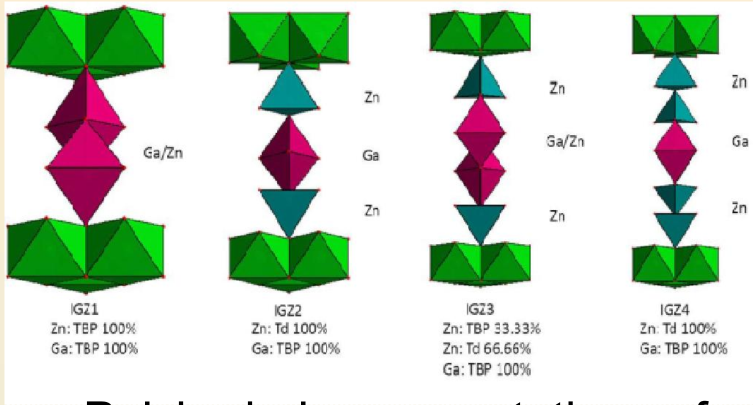

Polyhedral representations of **InGaO3(ZnO)m ;**
XRD representation

Problem:

No clarity regarding the exact geometries of Zn or Ga

Approach:

EXAFS spectroscopic measurements at the Zn & Ga K-edges(TBP to Td)

Soumya B. Narendranath, Ashok KumarYadav, T.G. Ajithkumar, Dibyendu Bhattacharyya, Shambu Nath Jha, Krishna K. Dey, Thirumalaiswamy Raja and R. Nandini Devi, *Dalton Trans., 43 (2014) 2120.*

………EXAFS of InGaO3(ZnO)m (m=1-4)

Paths	Parameters	m=1	m=2	m=3	m=4
Zn-O	R (Å)	1.91(±0.015)	1.91(±0.003)	1.89(±0.005)	1.91(±0.007)
	N	3(±0.03)	3.78(±0.024)	2.85(±0.039)	3.0(±0.08)
	σ^2	0.006(±0.001)	0.006(±0.001)	0.006(±0.001)	0.007(±0.001)
Zn-O	R (Å)	2.34(±0.001)	2.38(±0.018)	2.24(±0.018)	2.21(±0.02)
	N	2(±0.09)	0.91(±0.15)	1.37(±0.17)	0.96(±0.11)
	σ^2	0.009(±0.002)	0.005(±0.003)	0.01(±0.003)	0.003(±0.001)
Total O atoms		5	4.69	4.22	3.96

- Zn and Ga atoms are coordinated by 5 oxygen atoms for both m=1 and m=2 but for m=3 Zn and Ga atoms are surrounded by 4 oxygen atoms.

- One of the apical Ga-O bond is found unexpectedly large (2.135 Å) for m=2 which is results of position of Ga in the equatorial triangle of the trigonal bipyramid.

- There is no contribution of Ga-In shell in second peak since at higher m values the distance of the Ga-containing layer increase from the octahedral InO_2 layers.

- Coordination of the Ga-Zn shell decreases and that of the Ga-Ga shell increases for m=3 sample compared to that of the m=2 sample.

X-ray absorption spectroscopy of Sb doped Bi_2UO_6

Samples prepared at FCD, BARC

The BiO sheet resembles a fluorite structure where each Bi atom is coordinated by 4 in-plane oxygens (O_2 type) and three out of plane oxygens (O_3 type) which connects it to the UO_8 polyhedra.

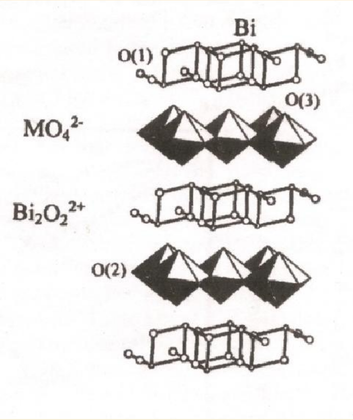

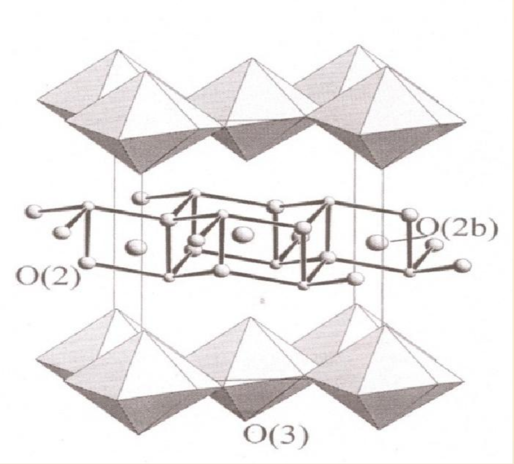

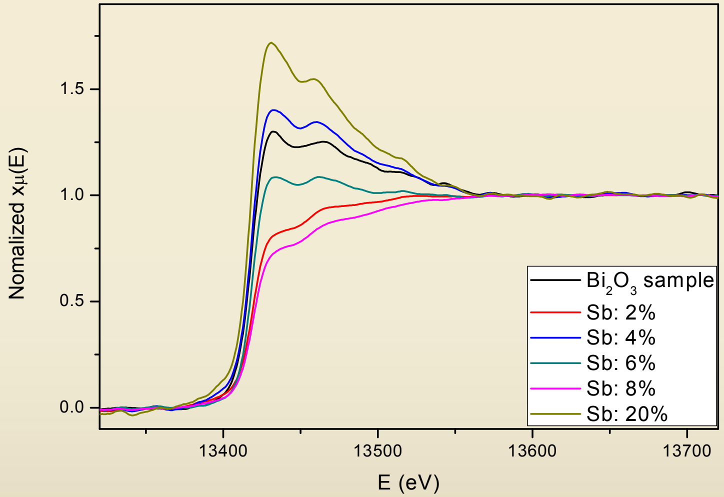

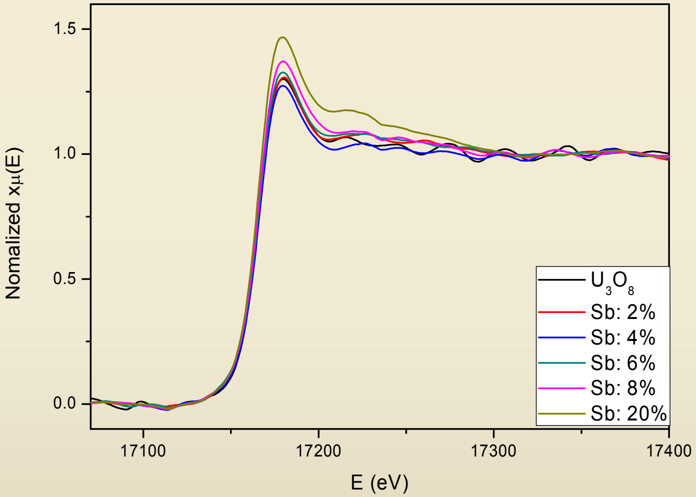

- **Sb doping does not alter the UO_8 polyhedra but Bi is substituted by Sb (similar ionic radius)**
- **The above result is consistent with the fact that Sb being more electronegative than Bi, Sb doping should increase effective positive charge at Bi sites.**

N. L. Misra, A. K. Yadav, Sangita Dhara, S. K. Mishra, Rohan Phatak, A. K. Poswal, S. N. Jha, A. K. Sinha and D. Bhattacharyya, Analytical Sciences, 29, 1-6, 2013.

XANES study

Chemical shift in Mn Compounds

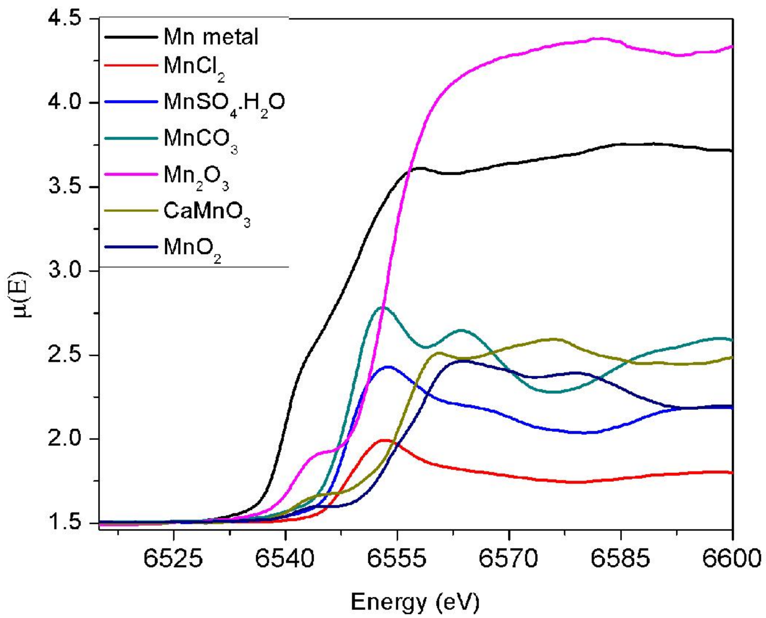

Chemical shift in Cr compounds

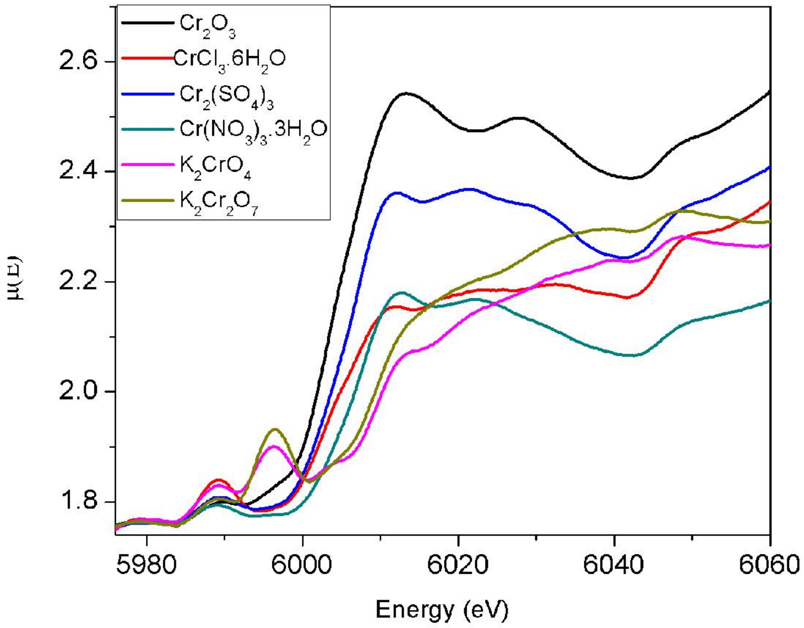

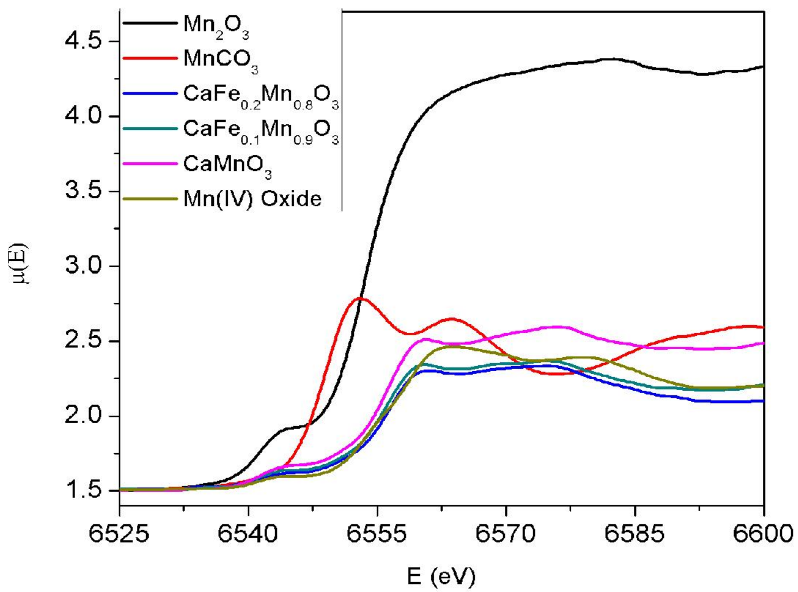

High resolution XANES study: Shift in absorption edge

(in collaboration with NPD, BARC)

Absorption edge shifts due to change in oxidation state and also due to change in anionic species/chemical environment : Effective Charge

D. Joseph, S. Basu, S.N. Jha and D. Bhattacharyya, Nuclear Instruments and Methods in Physics Research B 274 (2012) 126.

D. Joseph, A.K. Yadav, S.N.Jha and D.Bhattacharyya Bulletin of Materials Science (2012)

List of journal publications from the EXAFS beamlines at INDUS-2 SRS since 2009

1.	*Nature of WO4 tetrahedra in blue light emitting CaWO4 particles: Probed through EXAFS technique*	*RSC Adv., 2014(in Press)*
2.	*Nano-size effects on the nature of bonding in Y2Sn2O7: EXAFS and Raman spectroscopic investigations*	*Chemical Physics Letter597 (2014) 51*
3.	*Origin of giant dielectric constant and magnetodielectric study in Ba(Fe0.5Nb0.5)O3 nanoceramics*	*Journal of alloy and comp. 591(2014) 224.*
4.	*Chemical shift of U L3-edges in different Uranium compounds obtained by X-ray absorption spectroscopy*	*Bulletin of Materials Science (2014) in press.*
5.	*Effect of size and aspect ratio on structural parameters and evidence of shape transition in zinc oxide nanostructures*	*Journal of Physics and Chemistry of Solids 75(2014) 543.*
6.	*Correlation of structural and magnetic properties of Ni-doped ZnO nanocrystals*	*J. Phys. D: Appl. Phys. 47 (2014) 045308.*
7.	*Structural, optical and magnetic properties of sol–gel derived ZnO:Co diluted magnetic semiconductor nanocrystals:*	*J. Mater. Chem. C 2 (2014) 481.*
8.	*Investigations into variations in local cationic environment in layered oxide series $InGaO_3(ZnO)_m$ (m = 1-4)*	Dalton Transactions 43 (2014) 2120.
9.	*Surface strain engineering through Tb doping to study the pressure dependence of exciton-phonon coupling in ZnO NP*	J. Appl. Phys. 114 (2013) 214309.
10.	*Characterization of Sb-doped Bi_2UO_6 Solid Solutions by X-ray Diffraction and X-ray Absorption Spectroscopy*	Analytical Sciences 29 (2013) 579.
11.	*Chemical shift of Mn and Cr K-edges in X-ray absorption spectroscopy with Synchrotron Radiation*	Bulletin of Materials Science 36 (2013) 1067.
12.	*Probing local environments in Eu^{3+} doped $SrSnO_3$ nano-rods by luminescence and Sr K-edge EXAFS techniques*	Chem. Phys. Lett. 561–562 (2013) 82.
13.	*Extended X-ray Absorption Fine Structure (EXAFS) study of Gd doped ZrO_2 systems*	J. Appl. Phys. 113 (2013) 043508.
14.	*A comparative study of the spectra recorded at RRCAT synchrotron BL-8 dispersive EXAFS beamline with other beamlines*	Pramana 80 (2013) 159.
15.	*Transport and magnetic properties of Fe doped $CaMnO_3$*	J. Appl. Phys. 112 (2012) 123913.
16.	*One-pot thioetherification of aryl halides with thiourea and benzyl bromide in water catalyzed by Cu-grafted furfural imine functionalized mesoporous SBA-15*	Chem. Commun. 48 (2012) 8000.
17.	*XPS, EXAFS, and FTIR As Tools To Probe the Unexpected Adsorption-Coupled Reduction of U(VI) to U(V) and U(IV) on Borassus f labellifer-Based Adsorbents*	Langmuir 28 (2012) 16038.
18.	*X-ray Absorption Spectroscopy of doped ZrO_2 systems*	J. Appl. Phys. 111 (2012) 053532.
19.	*Eu^{3+} assisted structural collapse of GaOOH nanorods: Probed through EXAFS and vibrational technique*	Chem. Phys. Lett. 528 (2012) 21.
20.	*Chemical shifts of K-X-ray absorption edges on Copper in different compounds by X-ray Absorption Spectroscopy (XAS) with Synchrotron radiation*	Nuclear Inst. and Methods in Physics Research B 274 (2012) 126.
21.	*EXAFS measurements on $PbMoO_4$ crystals prepared under different conditions*	Bull. Mater. Sci. 35 (2012) 103.
22.	*EXAFS study of binuclear hydroxo-bridged copper (II) complexes*	*Journal of Coordination Chemistry 64 (2011) 1265.*
23.	*On the method of calibration of the energy dispersive EXAFS beamline at Indus-2 and fitting theoretical model to the EXAFS spectrum*	*Sadhana (India) 36 (2011) 339.*
24.	*First Results from a Dispersive EXAFS beamline developed at INDUS-2 Synchrotron Source at RRCAT, Indore, India*	*Nuclear Instruments Method. in Phys. Res. A 609 (2009) 286.*
25.	*X-ray Absorption Spectroscopy of PbMoO4 crystals*	*Bull. Mater. Sci. 32 (2009) 103.*

Summary

- XAFS is an extremely versatile technique for local structure probe.
- XAFS allows the determination of the oxidation state, the coordination motif of the probed element, the identity and the number of adjacent atoms and the absorber-ligand distances.
- Find applications in: Magnetic materials to Bioinorganic chemistry, catalyisis, envirnomental science, physics, material science etc.

❖Dispersive EXAFS beamline(BL-8) can be used for in-situ studies, kinetic catalysis etc.

❖Scanning EXAFS beamline can be used for dilute samples and thin film samples in fluorescence mode/transmission mode.

❖Sample environments available : 10K to 1000K

For booking beam time: register @
https://www.info-rrcat.ernet.in/beamline/

For details of beamline:
http://www.cat.gov.in/technology/accel/srul/beamlines/exafs.html

Collaborators

N.K. Sahoo
N.C.Das
D. Bhattacharyya
A.K.Poswal
A. Agarwal
S. Basu
A.K. Yadav
C. Nayak
P. Rajput

CDM, BARC

B.D. Srivastava & group
D.Lahiri
A.K.Tripathi & group
B.S. Tomar & group
D. Joseph
N.L. Mishra & group
Nandini devi, NCL, Pune
A. Das
A. Chakrabarty
& all other users of BL-8

Acknowledgements

ISUD, RRCAT
Director, Physics Group, BARC
Director, RRCAT
Director, BARC

Thank you